Failures Related to Heat Treating Operations

G.E. Totten, G.E. Totten & Associates, LLC
M. Narazaki, Utsunomiya University (Japan)
R.R. Blackwood and L.M. Jarvis, Tenaxol Inc.

HEAT TREATING—of all the various steel processing methods—has the greatest overall impact on control of microstructure, properties, residual stresses, and dimensional control. This article provides an overview of the effects of various material and process-related parameters on residual stress, distortion control, cracking, and microstructure/property relationships as they relate to various types of failure. The subjects that are discussed include:

- Phase transformations during heat treating
- Metallurgical sources of stress and distortion during heating and cooling
- Effect of materials and quench-process design on distortion and cracking
- Quenchant selection
- Effect of cooling characteristics on residual stress and distortion
- Methods of minimizing distortion
- Tempering
- Effect of the heat treatment process on microstructure/property-related failures, such as cracking

Phase Transformation during Heating and Cooling

Steel Transformation

Properties such as hardness, strength, ductility, and toughness are dependent on the microstructural products that are present in steel. The first step in the transformation process is to heat the steel to its austenitizing temperature. The steel is then cooled rapidly to avoid the formation of pearlite, which is a relatively soft transformation product; to maximize the formation of martensite, a relatively hard transformation product; and to achieve the desired as-quenched hardness.

The most common transformational products that may be formed from austenite in quench-hardenable steels are, in order of formation with decreasing cooling rate: martensite, bainite, pearlite, ferrite, and cementite. The formation of these products and the proportions of each are dependent on the time and temperature cooling history of the particular alloy and the elemental composition of that alloy. The transformation products formed are typically illustrated with the use of transformation diagrams, which show the temperature-time dependence of the microstructure formation process for the alloy being studied. Two of the most commonly used transformation diagrams are time-temperature-transformation (TTT) and continuous cooling transformation (CCT) diagrams.

Time-temperature-transformation diagrams, also called isothermal transformation diagrams, are developed by heating small samples of steel to the temperature where austenite transformation structure is completely formed, that is, the austenitizing temperature (T_A), and then rapidly cooling to a temperature intermediate between the austenitizing and the martensite start (M_s) temperature and then holding for a fixed period of time until the transformation is complete, at which point the transformation products are determined. This is done repeatedly until a TTT diagram is constructed, such as that shown for an unalloyed steel (American Iron and Steel Institute, or AISI, 1045) in Fig. 1. Time-temperature-transformation diagrams can only be read along the isotherms. The temperature A_1 is where transformation to austenite begins, and

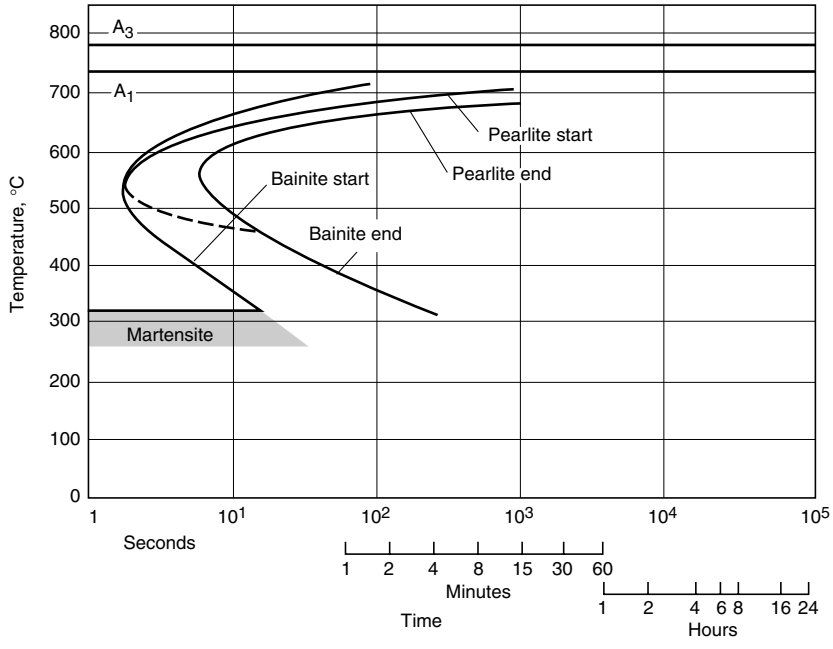

Fig. 1 Time-temperature-transformation diagram of an unalloyed steel containing 0.45% C. Austenitization temperature, 880 °C (1620 °F). The temperature A_1 is where transformation to austenite begins, and temperature A_3 is where the transformation to austenite is complete. Courtesy of Verlag Stahlessen mbH Dusseldorf

temperature A_3 is where the transformation to austenite is complete.

Continuous Cooling Transformation Diagrams. Alternatively, samples of a given steel may be continuously cooled at different specified rates, and the proportion of transformation products formed after cooling to various temperatures intermediate between the austenitizing temperature and the M_s may be determined in order to construct a CCT diagram, such as the one shown for an unalloyed carbon steel (AISI 1045) in Fig. 2. Continuous cooling transformation curves provide data on the temperatures for each phase transformation, the amount of transformation product obtained for a given cooling rate with time, and the cooling rate necessary to obtain martensite. The critical cooling rate is dictated by the time required to avoid formation of pearlite for the particular steel being quenched. As a general rule, a quenchant must produce a cooling rate equivalent to, or faster than, that indicated by the "nose" of the pearlite transformation curve in order to maximize martensite transformation product. Continuous cooling transformation diagrams can only be read along the curves of different cooling rates.

Caution: Although it is becoming increasingly common to see cooling curves (temperature-time profiles) for different quenchants, such as oil, water, air, and others, superimposed on either TTT or CCT diagrams, this is not a rigorously correct practice, and various errors are introduced into such analysis due to the inherently different kinetics of cooling used to obtain the TTT or CCT diagrams (described previously) versus the quenchants being represented. If a cooling curve is to be superimposed on a transformation diagram, a CCT, not a TTT, diagram should be used.

Metallurgical Crystal Structure

When steel is slowly cooled, it undergoes a crystal structure (size) change as it transforms from a less densely packed austenite (face-centered cubic, or fcc) to a more densely packed body-centered cubic (bcc) structure of ferrite. At faster cooling rates, the formation of ferrite is suppressed, and martensite, which is an even less densely packed body-centered tetragonal (bct) structure than austenite, is formed. Illustrations of these crystal structures are provided in Fig. 3. This results in a volumetric expansion at the M_s temperature, as shown in Fig. 4.

Figure 5 shows that the crystal lattice of austenite expands with increasing carbon content (Ref 1). It has been reported that, typically, when a carbide-ferrite mixture is converted to martensite, the resulting expansion due to increasing carbon content is approximately 0.002 in./in. at 0.25% C and 0.007 in./in. at 1.2% C (Ref 1). The fractional increase in size when austenite is converted to martensite is approximately 0.014 in./in. for eutectoid compositions. This illustrates the effect of carbon structure and steel transformation on residual stresses and distortion leading to dimensional changes.

Estimation of Volumetric Change due to Steel Transformation

In the previous discussion, it has been shown that there are various microstructures possible on heating and cooling of steel, and that the potential microstructural transformations that are possible for a given steel are illustrated by their CCT or TTT diagrams. Furthermore, dimensional changes are possible, depending on the carbon content and microstructural transformation product formed. Table 1 summarizes the atomic volumes of different microstructural components as a function of carbon content (Ref 2). Table 2 provides an estimate of volumetric changes as a function of carbon content for different metallurgical transformations (Ref 3, 4).

Volumetric expansion occurring as a result of quenching can be estimated from (Ref 5):

$$\Delta V/V \times 100 = (100 - V_c - V_a) \times 1.68C + V_a(-4.64 + 2.21C) \quad \text{(Eq 1)}$$

where $(\Delta V/V) \times 100$ equals the percentage change in volume, V_c equals the percentage by volume of undissolved cementite, $(100 - V_c - V_a)$ equals the percentage by volume of martensite, V_a equals the percentage by volume of austenite, and C equals the percentage by weight of carbon dissolved in austenite and martensite.

If the value of $(\Delta V/V)$ is known or can be computed, then internal stresses that are developed in a part due to temperature differences (ΔT) arising from either one-dimensional heating or cooling can be estimated from (Ref 6):

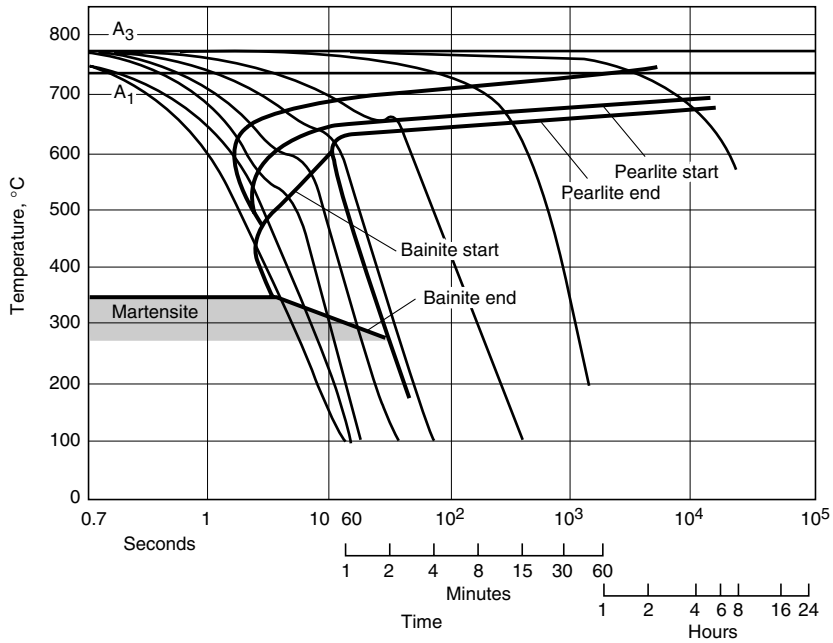

Fig. 2 Continuous cooling transformation diagram of an unalloyed steel containing 0.45% C. Austenitization temperature, 880 °C (1620 °F). Courtesy of Verlag Stahlessen mbH Dusseldorf

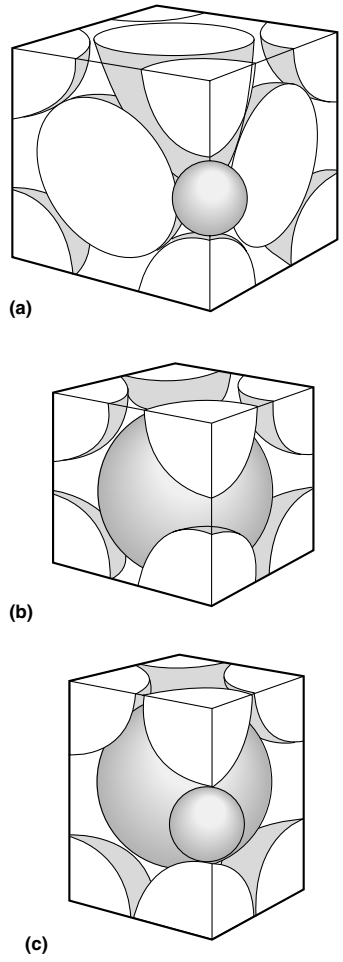

Fig. 3 Crystal structures. (a) Austenite (fcc). (b) Ferrite (bcc). (c) Martensite (bct)

$$\sigma = E \cdot \varepsilon = E \cdot \tfrac{1}{3}(\Delta V/V) = E \cdot \alpha \cdot \Delta T \qquad \text{(Eq 2)}$$

where σ is stress, ε is strain, E (modulus of elasticity) $= 2 \times 10^5$ N/mm^2, and α (coefficient of thermal expansion) $= 1.2 \times 10^{-5}$. Relative volume changes due to phase transformation are illustrated in Fig. 6 (Ref 6).

Figure 7 shows that stresses, such as an increase in hydrostatic pressure, accelerate phase transformations (Ref 7). This occurs whether the stresses are tensile or compressive and results in accelerated austenite decomposition and increased M_s temperature. The strain of this process is often estimated as being equal to the volumetric expansion divided by 3 (Ref 8). Transformation plasticity is a process whereby a stress affects linear strain. This is illustrated in Fig. 8, where the effect of applied stress on martensitic transformation strain is shown (Ref 8). Generally, the M_s temperature is increased by tensile stress and decreased by hydrostatic pressure. Figure 9 shows that stress exhibits very large effects on the start and stop times for pearlitic transformation (Ref 7).

Cooling and Steel Metallurgical Transformation

Cooling without Transformation (Ref 6, 7). If steel is cooled sufficiently fast, cooling is not accompanied with microstructural transformation changes. Under these conditions, the surface of the component cooled much more quickly than the core at first, as illustrated in Fig. 10 (Ref 9). At this point, the specific volume in the core is greater than that of the surface, and the reduction in volume at the surface (due to lower temperature) is resisted by the greater volume in the core, resulting in the surface being in tension and the core in compression.

At the point of maximum temperature difference between the surface and the core (point T), the core cools (shrinks) more quickly than the surface, leading to an elastic dimensional reduction of the surface until a point of stress conversion is obtained, at which point the surface is in compression relative to the core. After the cooling processes have been completed, the residual stress distribution between the surface and the core, shown at the bottom right in Fig. 10 (Ref 9), is obtained. If the surface stresses exceed the hot yield strength of the material, it plastically deforms, resulting in thermally induced dimensional changes.

Cooling with Transformation (Ref 6, 7). When steels that may undergo transformational changes are quenched, the possibility of the formation of both thermal and transformational stresses must be considered. Figure 11 illustrates three different examples of this process (Ref 8).

Example 1, illustrated in Fig. 11(a), occurs when phase transformation of both the surface and the core occurs before the thermal stresses change sign. Above the M_s transformation temperature, the stresses that are formed are thermal. On further cooling, the stresses in the core exceed the yield strength, and plastic deformation (elongation) occurs. Subsequent martensitic transformation at the core provides a substantial stress component, due to volumetric increases from martensitic phase transformation. This causes the core to be in compression and the surface to be in tension simultaneously.

Example 2 (Fig. 11b) illustrates the case that begins after the thermal stresses change sign. The transformation-induced volume increase of the surface layer adds to the compressive stresses at the surface. Because the stresses are balanced, there is a corresponding increase in the tensile stresses in the core.

Example 3 is a case where, although the transformation of the core starts later, it finishes before the surface (Fig. 11c). During the cooling process, the sign of the stresses changes three times. There are important consequences whether the core transforms before or after the stress reversal, because thermal stresses may be counteracted, and tensile surface residual stresses may result when the core transforms after the surface and before the stress reversal (Ref 8).

This is illustrated, in Fig. 12. If the steel transformation occurs before the thermal stress maximum (sequence 4 in Fig. 12), the ferrite/pearlite structure of a cylindrical test specimen is distorted into a barrel shape (Ref 6). If the transformation occurs after the thermal stress maximum (sequence 1 in Fig. 12), the austenite is pressed into a barrel shape, followed by a volumetric increase due to martensitic transformation. This results in high tensile residual stresses on the surface. If the steel transformation occurs simultaneously with the maximum thermal stresses, transformation in the core occurs prior to surface transformation (sequence 3 in Fig. 12), and a barrel shape appears with high compressive stresses on the surface. If the surface is transformed prior to the core (sequence 2 in Fig. 12), the transformational stresses decrease or possibly even reverse the thermal stresses. If this occurs, a spool shape is formed.

These data show that the position of cooling curves for both the surface and the core for the quenching process must be considered with the appropriate TTT curve for the steel of interest, and that there are numerous mixtures of thermal and transformational stresses possible. Table 3 provides a summary of these processes (Ref 6).

In some steels, those with higher carbon content and alloy steels, the M_f temperature is below 32 °F (0 °C), which means that it is likely that at the conclusion of the heat treating process there is as much as 5 to 15% of austenite remaining (Ref 10). The amount of retained austenite exhibits significant effects on the magnitude of compressive stresses formed and, ultimately, on

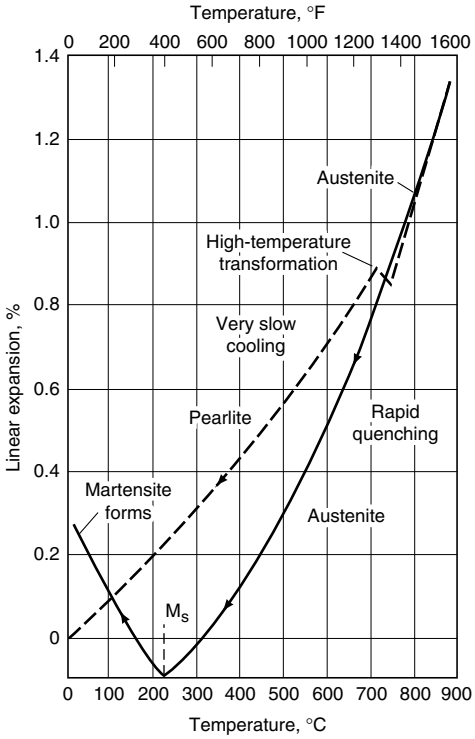

Fig. 4 Steel expansion and contraction on heating and cooling

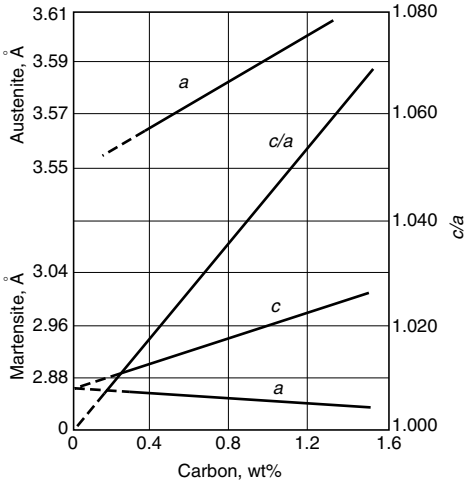

Fig. 5 Carbon content versus lattice parameters of (retained) austenite and martensite at room temperature. *a* at the top of the graph is the lattice parameter of fcc austenite. *a* and *c* in the lower half of the graph are the lattice parameters for tetragonal martensite. The ratio of *c/a* for martensite as a function of carbon content is also given.

Table 1 Atomic volumes of selected microstructural constituents of ferrous alloys

Phase	Apparent atomic volume, Å^3
Ferrite	11.789
Cementite	12.769
Ferrite + carbides	11.786 + 0.163 C(a)
Pearlite	11.916
Austenite	11.401 + 0.329 C(a)
Martensite	11.789 + 0.370 C(a)

(a) C = % carbon

dimensional changes to be expected. Some of the factors affecting retaining austenite formation include chemical composition (which dictates the M_s temperature), quenching temperature, quenching cooling rates, austenitizing temperature, grain size, and tempering.

Tempering

Steel parts are often tempered by reheating after quench hardening to obtain specific values of mechanical properties. Tempering of steel increases ductility and toughness of quench-hardened steel and also relieves quench stresses and ensures dimensional stability. The tempering process involves heating hardened steel to some temperature below the eutectoid temperature for the purposes of decreasing hardness and increasing toughness. In general, the tempering process is divided into four stages, which are summarized in Table 4 (Ref 9). These include (Ref 11, 12):

1. Tempering of martensite structure
2. Transformation of retained austenite to martensite
3. Tempering of the decomposition products of martensite and at temperatures above 480 °C (900 °F)
4. Decomposition of retained austenite to martensite

Figure 13 illustrates the effect of microstructural variation during tempering on the volume changes occurring during the tempering of hardened steel (Ref 9).

Figure 14 illustrates the effect of dimensional variation and retained austenite content of a bearing steel (100Cr6) as a function of tempering temperature (Ref 10). Tempering may also lead to dimensional variation due to relaxation of residual stresses and plastic deformation, which is due to the temperature dependence of yield strength (Ref 11).

In addition to dimensional change by microstructural variation, tempering may also lead to dimensional variation due to relaxation of residual stresses and plastic distortion, which is due to the temperature dependence of yield strength (Ref 13). Figure 15 shows the distortion of round steel bars (200 mm, or 8 in., in diameter and 500 mm, or 20 in., in length) by quenching and by stress relieving by tempering. A medium-carbon steel bar (upper diagrams) and a hardenable steel bar (lower diagrams) are used in this experiment. Figures 15(a) and (d) are the results of quenching from 650 °C (1200 °F) without phase transformation. The distortion in each case is almost the same, regardless of the different quenchants and the different chemical compositions. These convex distortions are caused by nonuniform thermal contraction and resultant thermal stress during cooling. Figures 15(b) and (e) are the results of quenching from 850 °C (1560 °F) with phase transformation. The distortion in Fig. 15(e) (hardenable steel) shows a convex configuration, but the distortion in Fig. 15(b) (medium-carbon steel of poor hardenability) shows a configuration that combines convex and concave distortion. In addition, water quenching has a greater effect on distortion than oil quenching. Figures 15(c) and (f) show the configurations after tempering. These results show that tempering after quenching results in not only volumetric changes but also convex distortions. Such distortions seem to be related to relieving of residual stresses by tempering.

Figure 16 and 17 (Ref 14) show the example of stress relief by tempering. A solid cylinder, 40 mm (1.6 in.) in diameter and 100 mm (4 in.) in length, was examined for analyses and experiments of tempering performed after water quenching. Calculated residual stress distributions after water quenching are illustrated in Fig. 16. Open and solid circles in the figure correspond to measured stresses on the surface of the cylinder by x-ray diffraction technique. Residual stress distributions after tempering at 400 °C (750 °F) are shown in Fig. 17(a) and (b) for typical elapsed times of 2 and 50 h, with measured values on the surface. These results show that the stresses in all directions decrease with elapsed time in tempering.

The following are recommendations with respect to the tempering process (Ref 4):

- Generally, the higher the tempering temperature, the greater the resulting ductility and toughness. However, this is at the expense of strength and hardness.
- High-carbon steels that contain appreciable amounts of retained austenite undergo an increase in hardness when tempered at approximately 230 °C (450 °F) as a result of decomposition of the austenite.
- Steel tempered at approximately 260 °C (500 °F) undergoes a loss of toughness (Fig. 18) that is associated with the formation of carbide films around prior martensite plates.
- Alloy steels undergo temper brittleness or a reduction in toughness that occurs when the steel is tempered in (or slowly cooled through) the temperature range of 510 to 593 °C (950 to 1100 °F). This phenomenon does not occur in plain carbon steels, but the degree of embrittlement is enhanced by nickel, manganese, and chromium content. Tempering should be carried out below this range for steels susceptible to this embrittlement or above the range, followed by rapid quenching through the range. Molybdenum additions minimize the susceptibility of steels to this form of embrittlement.
- Highly alloyed steels, for example, high-speed steels, many contain large amounts of retained austenite that is stable during tempering but transforms to brittle martensite on cooling from tempering. A second temper is then necessary to temper this brittle secondary martensite.

Metallurgical Sources of Stress and Distortion during Reheating and Quenching

Basic Distortion Mechanism. Shape and volume changes during heating and cooling can be attributed to three fundamental causes (Ref 15):

- Residual stresses that cause shape change when they exceed material yield strength. This occurs on heating when the strength properties decline.

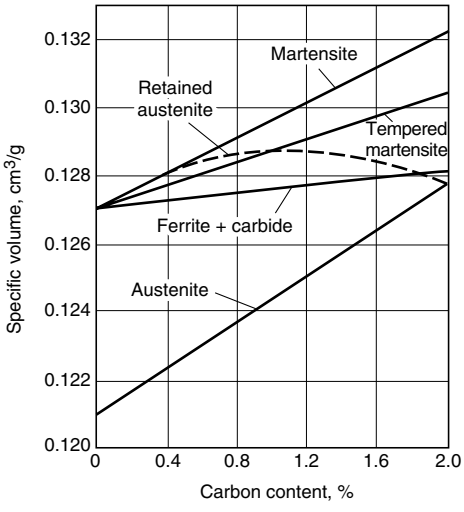

Fig. 6 Specific volume ($\Delta V/V$) of carbon steels relative to room temperature. Tempered martensite, <200 °C (390 °F)

Table 2 Size changes during hardening of carbon tool steels

Reaction	Volume change, %	Dimensional change, in./in.
Spheroidite → austenite	−4.64 + 2.21 (%C)	0.0155 + 0.0074 (%C)
Austenite → martensite	4.64 − 0.53 (%C)	0.0155 − 0.00118 (%C)
Spheroidite → martensite	1.68 (%C)	0.0056 (%C)
Austenite → lower bainite (a)	4.64 − 1.43 (%C)	0.0156 − 0.0048 (%C)
Spheroidite → lower bainite (a)	0.78 (%C)	0.0026 (%C)
Austenite → aggregate of ferrite and cementite (b)	4.64 − 2.21 (%C)	0.0155 − 0.0074 (%C)
Spheroidite → aggregate of ferrite and cementite (b)	0	0

(a) Lower bainite is assumed to be a mixture of ferrite and epsilon carbide. (b) Upper bainite and pearlite are assumed to be mixtures of ferrite and cementite.

- Stresses caused by differential expansion due to thermal gradients. These stresses increase with the thermal gradient and cause plastic deformation as the yield strength is exceeded.
- Volume changes due to transformational phase change. These volume changes are contained as residual stress systems until the yield strength is exceeded.

Relief of Residual Stresses. If a part has locked-in residual stresses, these stresses can be relieved by heating the part until the locked-in stresses exceed the strength of the material. A typical stress-strain curve obtained from a tension test is shown in Fig. 19 (Ref 15). Initial changes in shape are elastic, but under increased stress, they occur in the plastic zone and are permanent. On heating, the stresses are gradually relieved by changes in the shape of the part due to plastic flow. This is a continuous process, and as the temperature of the part is increased, the material yield stress decreases, as shown in Fig. 20 (Ref 16). It is a function not only of temperature but also of time, because the material creeps under lower applied stresses. It is apparent that the stresses can never be reduced to zero, because the material always possesses some level of yield strength below which residual stresses cannot be reduced.

Volume Changes during Phase Transformations. When a steel part is heated, it transforms to austenite, with an accompanying reduction in volume, as shown in Fig. 21 (Ref 17). When it is quenched, the structure transforms from austenite to martensite, and its volume increases. If these volume changes cause stresses to be set up that are constrained within the strength of the material, a residual stress system is created. If the stresses cannot be contained, then material movement occurs, which causes cracking under extreme conditions. The expansion is related to the composition of the steel. Figure 21 shows the relative volume increase of two steels as a function of austenitizing temperature and specimen dimensions.

While these physical changes are well known, the situation is made more complex when all three events occur simultaneously. In addition, other events, such as heating rate, quenching, and inconsistent material composition, further complicate the process.

When parts are heated during heat treatment, a thermal gradient exists across the cross section of the component. If a section is heated so that a portion of the component becomes hotter than the surrounding material, the hotter material expands and occupies a greater volume than the adjacent material and is thus exposed to applied stresses that cause a shape change when they exceed material strength. These movements can be related to heating rate and section thickness of the component.

Effect of Materials and Process Design on Distortion

Quenchant selection and quenching conditions are critically important parameters in quench system design. For example, one study compared the distortion obtained when a 0.4% medium-carbon plain steel bar 200 mm (8 in.) in diameter by 500 mm (20 in.) long is quenched in water or oil from 680 °C (1260 °F) (Ref 18, 19). The results, Fig. 22(a) and (c), show that essentially equivalent variation in diameter and length with both cooling processes was obtained, which was due to thermal strains within the steel. Interestingly, the well-known diameter variations at the end of the bar, known as the "end-effect," were observed, which is attributable to heat extraction from both the sides and ends of the bar.

If the same steel bars of the same dimensions are heated to 850 °C (1560 °F) to austenitize the steel and then quenched in water or oil, the results shown in Fig. 22(b) and (d), respectively, were obtained (Ref 18, 19). Considerably greater dimensional variation and lengthening of the bar (for the oil quench) was obtained due to both thermal and transformational strains with the steel.

The dimensional changes of a 70 mm (2.75 in.) steel (0.15% C, 1% Mn, 0.75% Cr, 0.85% Ni) cube were modeled after austenitizing and then quenching in water and oil (Ref 18, 20). The results of this work are shown in Fig. 23. As seen in the figure, the edges and faces shrink (becoming concave), and the effects are greater when

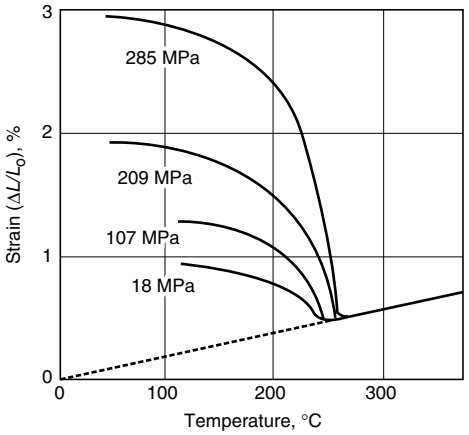

Fig. 8 Dilatometer curves for a 0.6% carbon steel (60NCD11) for different applied stresses

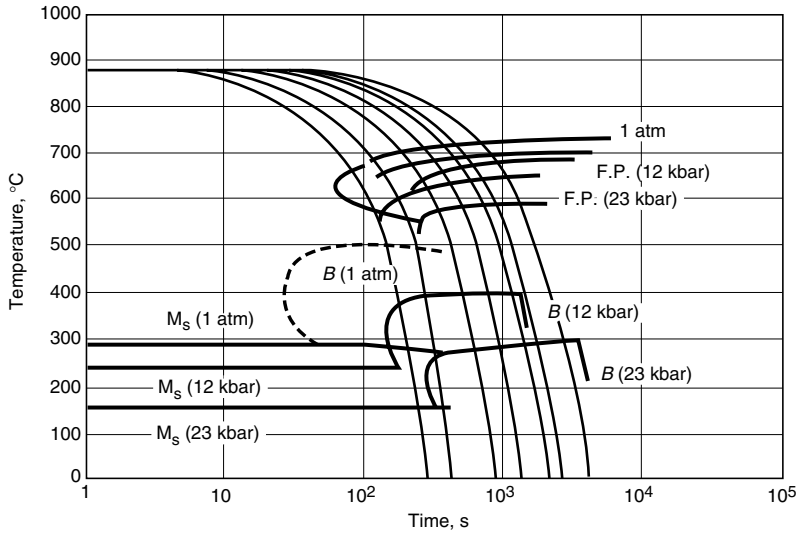

Fig. 7 Effect of hydrostatic pressure on the transformation kinetics of 50CV4 steel. *B*, bainite; F. P., ferrite-pearlite transformation; M_s, martensite start temperature. Source: Ref 7

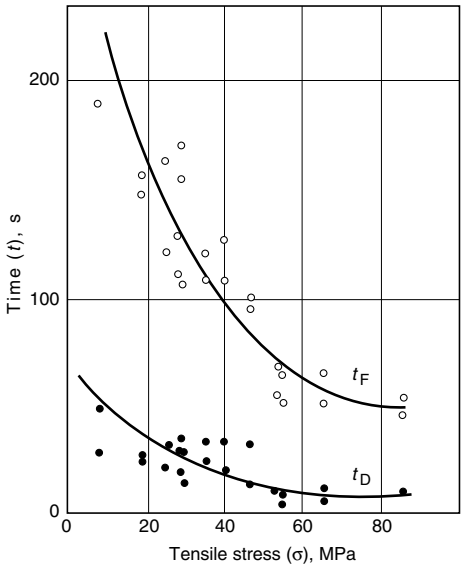

Fig. 9 Effect of tensile stress on pearlite transformation starting and ending times. Isothermal transformation at 673°C (1243 °F), eutectoid steel. The t_D and t_F times are transformation starting and ending times, respectively.

the steel is quenched in water than when it is quenched in oil.

There are various factors that can affect distortion and growth of steel in heat treating. These include component design, steel grade and condition, machining, component support and loading, surface condition, heating and atmosphere control, retained austenite, and the quenching process (Ref 21).

Component Design. One of the overwhelming causes of steel cracking and unacceptable distortion control is component design. Poor component design promotes distortion and cracking by accentuating nonuniform and nonsymmetrical heat transfer during heating and cooling. Component design characteristics that are common to distortion and cracking problems include (Ref 22, 23):

- Parts that are long, with thin cross sections. Long and thin parts are defined as those greater than $L = 5d$ for water quenching, $L = 8d$ for oil quenching, and $L = 10d$ for austempering, where L is the length of the parts, and d is the thickness or diameter. Long and thin parts may be quenched using a support mechanism, such as that illustrated in Fig. 24.
- Parts that possess large cross-sectional area (A) and are thin (t), which are defined as $A = 50t$.

Parts that exceed these dimensions often must be straightened or press quenched to maintain dimensional stability (Ref 23). If possible, materials with sufficient hardenability should be oil or salt quenched. A schematic illustration of a press quenching system is provided in Fig. 25.

The following are additional guidelines (Ref 4):

- Balance the areas of mass.
- Avoid sharp corners and reentrant angles.
- Avoid sharp corners between heavy and thin sections.
- Avoid single internal or external keys, keyways, or splines.
- Provide adequate fillet or radius at the base of gear teeth, splines, and serrations.
- Do not have holes in direct line with the sharp angles of cutouts.
- Avoid a sharp corner at the bottom of small openings, such as in drawing or piercing dies, because spalling or flaking is likely to result at these points.
- Keep hubs of gears, cutters, and so on as near the same thickness as possible, because dishing is likely to occur.

Additional design considerations to reduce the probability of distortion, cracking, and soft spots include (Ref 4):

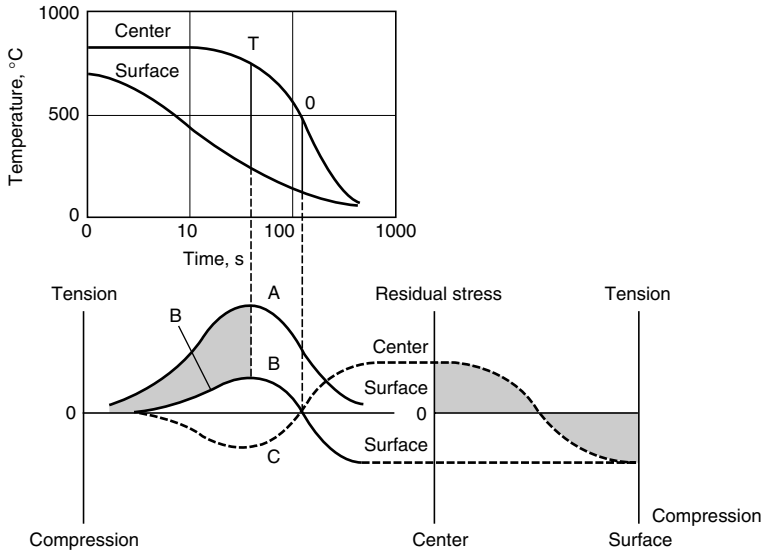

Fig. 10 Development of thermal stresses within steel on cooling. T, time instant at maximum temperature difference; 0, time instant of stress reversal; curve A, stress variation at the surface under elastic conditions. B and C are actual thermal stress variations at the surface and the core under elastic-plastic conditions.

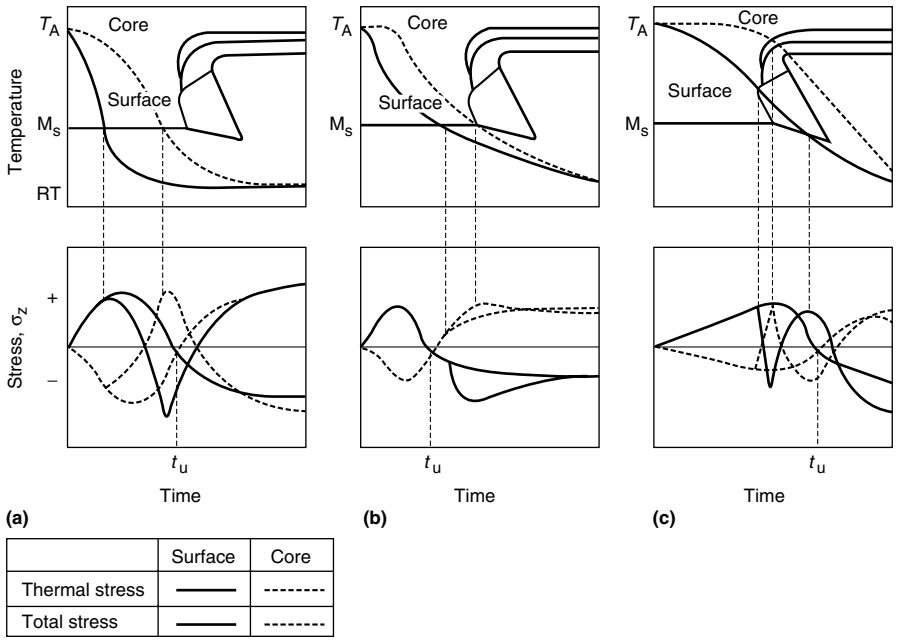

	Surface	Core
Thermal stress	———	- - - - - - -
Total stress	———	- - - - - - -

Fig. 11 Comparison of thermal and transformational stresses for three different quenching conditions. See text for details. t_u, time instant of stress reversal

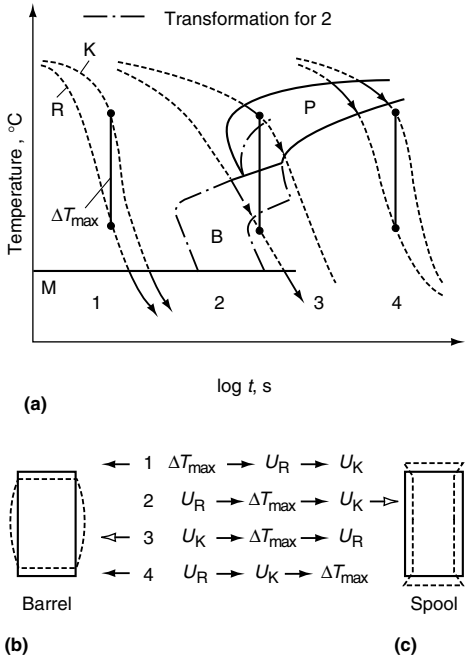

Fig. 12 Size change due to thermal changes and phase transformation. K, core; R, surface

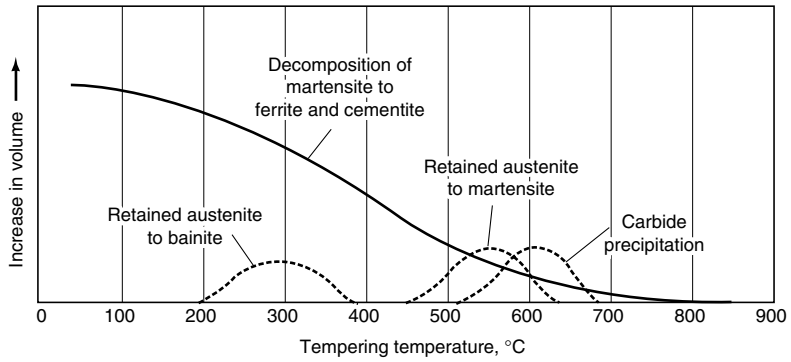

Fig. 13 Effect of microstructural constitutional variation on volume changes during tempering

- Order stock large enough to allow for machining to remove decarburized surfaces and surface imperfections, such as laps and seams.
- Do not drill screw holes closer than 6.35 mm (0.25 in.) from edges of die blocks or large parts, where possible. Cracking may be avoided by using steel that may be hardened by using lower quench severity, or if possible, pack the bolt hole to reduce thermal stresses arising due to quenching.
- Avoid blind holes, if possible.
- All parts should be designed with round corners and fillets wherever possible.
- Use air-hardening or high-carbon (oil- and air-hardening) tool steel on unbalanced and intricately shaped dies.
- Add extra holes, if possible, on heavy, unbalanced sections to allow for faster and more uniform cooling when quenched.
- Do not machine knife blades to a sharp cutting edge before hardening.
- Avoid deep scratches and tool marks.
- On long, delicate parallels, shafts, and so on, rough out and have pieces annealed to remove stresses before finish machining.
- Always use the grade or composition of steel most suitable for the work that the part has to perform.

A well-designed part is the best ensurance against breakage in hardening.

Design symmetry is also an important variable to minimize distortion. For example, the unsymmetrical gear design shown in the upper diagram of Fig. 26 typically may undergo distortion, as shown in the lower diagram of Fig. 26 (Ref 22). (The load on a gear tooth increases as a power of 4.3 with the taper [Ref 22]). The solution to the gear design problem shown in Fig. 26 is to provide greater symmetry, as shown in Fig. 27. If this is not possible, press quenching or tooth-by-tooth induction hardening may be the best alternative (Ref 22, 23).

Another common design problem occurs with parts having holes, deep keyways, and grooves. One illustration of this problem is hardening of a shaft over a lubrication cross hole, as illustrated in Fig. 28 (Ref 22). Preferred alternative designs are also shown in Fig. 28. If a radial cross hole is mandatory, the use of carburized steel with oil quenching would be preferred.

The distortion encountered when quenching a notched part, such as a shaft with a milled slot, is illustrated in Fig. 29 (Ref 23). In this case, nonuniform heat transfer results. The metal within the notch is affected by the shrinkage of the metal around it, due to slower cooling within the slot caused by vaporization of the quenchant. Therefore, on cooling, the metal on the side with the shaft is "too short," pulling the shaft out of alignment. A general rule for solving such quench distortion problems is that the "short side is the hot side," which means that the inside of the bowed metal was quenched more slowly than the opposite side (Ref 23).

Figure 30 provides an illustration of recommended design corrections that reduce the possibility of quench-cracking (Ref 4). If it is unavoidable that quench crack-sensitive designs be used, then two possible design modifications should be considered. The first is to consider a two-piece assembly that is mechanically joined

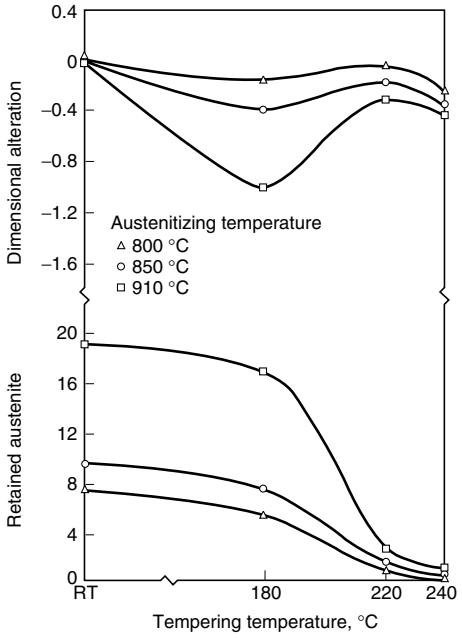

Fig. 14 Dimensional variation and retained austenite content of 100Cr6 steel as a function of tempering temperature

Table 3 Size change and residual stress caused by heat treatment of prismatic parts

	(Δ*T*)(a)	(Δ*V*/*V*)(b)	Dimensional dependency	(Δε)(c)	(σE)(d)	Example
Change of microstructure	Small	≠0	$\varepsilon_1 = \varepsilon_{11} = \varepsilon_{111}$	0	0	Tempering, precipitation hardening, isotropic material
Thermal stress	Big	0	$\varepsilon_1 < \varepsilon_{11} < \varepsilon_{111}$	>0	<0	Quenching of austenitic steels
Thermal and transformation stress						
Transformation R + K ***after*** thermal stress maximum	Small	>0	$\varepsilon_1 \sim \varepsilon_{11} \sim \varepsilon_{111}$	0	≫0	In air; full hardness penetration
	Big	≫0	$\varepsilon_1 < \varepsilon_{11} < \varepsilon_{111}$	>0	≫0	In water; full hardness penetration
Transformation R ***before*** K ***after*** thermal stress maximum	Big	>0	$\varepsilon_1 > \varepsilon_{11} > \varepsilon_{111}$	<0	>0	Medium hardness penetration
Transformation R ***before*** K ***after*** thermal stress maximum	Big	≥0	$\varepsilon_1 \ll \varepsilon_{11} \ll \varepsilon_{111}$	≫0	≪0	Shallow hardness penetration (shell hardening)
Transformation ***before*** R + K thermal stress maximum	Small	~0	$\varepsilon_1 \approx \varepsilon_{11} \approx \varepsilon_{111}$	0	~0	Normalizing, quenching without hardening
	Big	~0	$\varepsilon_1 < \varepsilon_{11} < \varepsilon_{111}$	>0	<0	

R, surface; K, core. (a) $\Delta T = (T_K - T_R)$. (b) $\Delta V/V$, relative volume change. (c) Convexity $\Delta\varepsilon = \varepsilon_k - \varepsilon_m$; ε_m, ε_k, dimensional change in middle of the plane. (d) σ_E, residual stress at the surface (remaining stress)

Table 4 Metallurgical reactions occurring at various temperature ranges and related physical changes of steel during tempering

Stage	Temperature range °C	Temperature range °F	Metallurgical reaction	Expansion/contraction
1	0–200	32–392	Precipitation of ε-carbide. Loss of tetragonality	Contraction
2	200–300	392–572	Decomposition of retained austenite	Expansion
3	230–350	446–662	ε-carbides decompose to cementite	Contraction
4	350–700	662–1292	Precipitation of alloy carbides. Grain coarsening	Expansion

Source: Ref 9

or shrunk-fitted together. The second is to manufacture the part from steel that can be hardened by martempering or by air cooling. These alternative design strategies produce lower stress and minimize cracking.

Steel Grade and Condition. Although steel cracking is most often due to nonuniform heating and cooling, material problems may be encountered. Some typical material problems include (Ref 22):

- The compositional tolerances should be checked to ensure that the alloy is within specification.
- Some alloys are particularly problematic. For example, some steel grades must be water quenched when the alloy composition is on the low side of the specification limit. Conversely, if the alloy composition is on the high side, cracking is more common. Steel grades that exhibit this problem include: 1040, 1045, 1536, 1541, 1137, 1141, and 1144. As a rule, steels with carbon contents and hardenability greater than 1037 are difficult to water quench (Ref 22).
- Some steel grades with high manganese are prone to microsegregation of manganese, gross segregation of chromium, and thus are prone to cracking. These include 1340, 1345, 1536, 1541, 4140, and 4150. If possible, it is often a good choice to replace the 4100 series with the 8600 series of steels (Ref 24).
- "Dirty" steels, those containing greater than 0.05% S (such as 1141 and 1144), are more prone to cracking. One reason for this is the greater alloy segregation in dirty steels, leading to alloy-rich and alloy-lean regions. Another reason is that these steels typically have a greater number of surface seams, which act as stress raisers. Also, dirty steels and steels with higher sulfur levels are often manufactured to coarse-grain practice for improved machinability; this also imparts greater brittleness and propensity for cracking.
- Decarburization of up to 0.06 mm (0.0025 in.) per 1.6 mm (1/16 in.) diameter may be present.

It is well known that cracking propensity increases with carbon content. Therefore, the carbon content of the steel is one of the determining factors for quenchant selection. Table 5 summarizes some average carbon-content concentra-

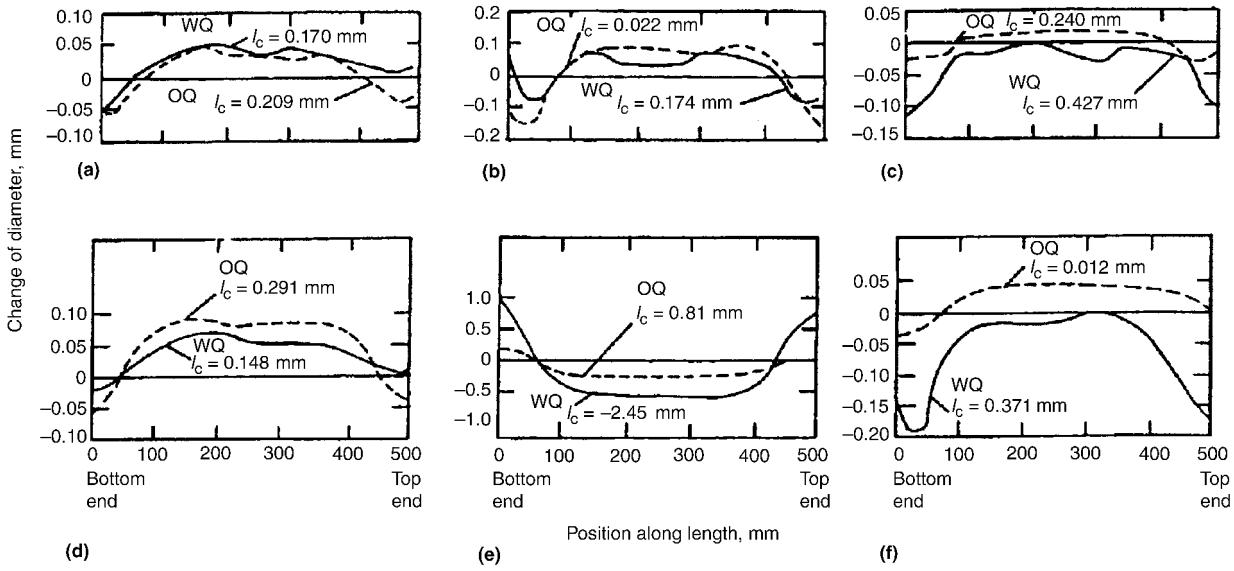

Fig. 15 Deformation of medium-carbon and hardenable steel bars by quenching from below and above the transformation temperature and by stress relieving. l_c, change of length; WQ, water quench; OQ, oil quench. (a) to (c) JIS S38C steel (0.38% C). (d) to (f) JIS SNCM 439 steel (0.39% C, 1.8% Ni, 0.8% Cr, 0.2% Mo). (a) and (d) Quenched from 650 °C (1200 °F). (b) and (e) Quenched from 850 °C (1560 °F). (c) and (f) Tempered at 650 °C (1200 °F)

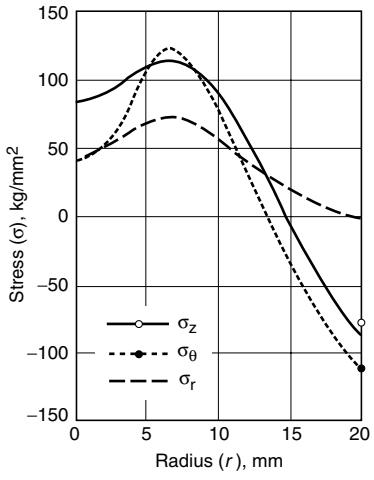

Fig. 16 Stress distribution in a cylinder after quenching

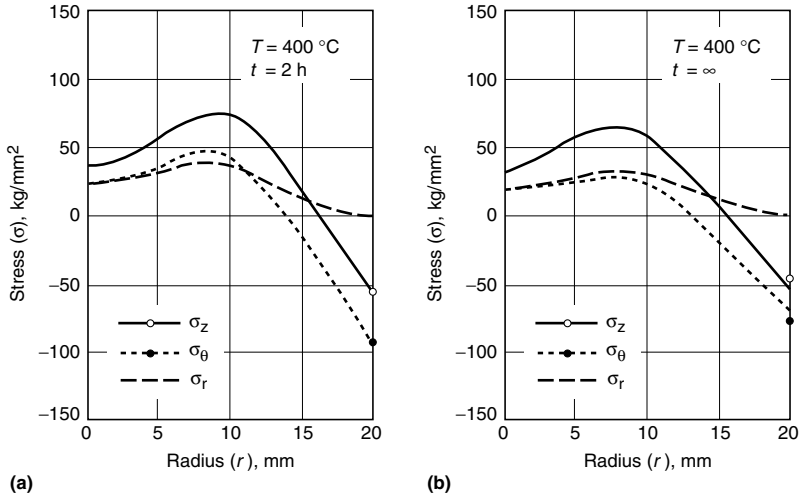

Fig. 17 Stress distribution in a cylinder after tempering. (a) $t = 2$ h. (b) Assume $t = \infty$.

tion limits for quenching steel into water, brine, or caustic (Ref 24).

Higher-carbon steels undergo greater expansion on hardening, and because the M_s temperature decreases with carbon content, expansion that does occur during martensitic transformation does so at a lower temperature, where the cracking of the steel is more likely than distortion. Therefore, cracking is more likely when hardening high-carbon steels than when heat treating low- or medium-carbon steels. As a rule of thumb, plain carbon steels with less than 0.35% C rarely crack on hardening, even under severe quenching conditions (Ref 4). The carbon content of a steel should never be greater than necessary for the specific application of the part.

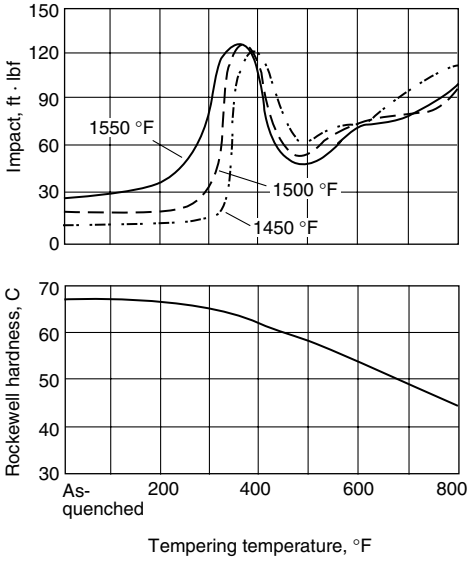

Fig. 18 The 260 to 315 °C (500 to 600 °F) impairment in torsion toughness in very hard steels. Note: Reduction in toughness is not detected by hardness measurements. Source: Ref 4

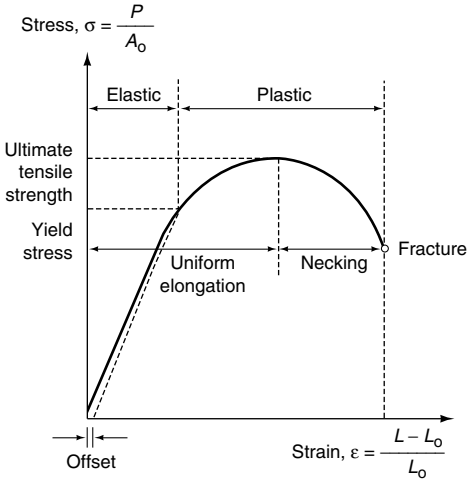

Fig. 19 Various features of a typical stress-strain curve obtained from a tension test

It is well known that regions containing high concentrations of coarse carbide microstructure as a result of improper forging may become the initiation point for subsequent quench cracking, particularly with parts of complex shape (Ref 25). It is important to provide a sufficient forging reduction ratio to allow the carbide formation to become fine and uniform (Ref 26).

Because part manufacture, such as gear production, often requires machining, the condition of the steel that is going to be machined is critically important. Some workers have recommended that normalized and subcritical annealed steel is the ideal condition (Ref 21). Subcritical annealing is performed to relieve stresses incurred during normalization without softening or homogenizing the steel. The subcritical annealing process reduces the carbon content and alloy carbide content in the austenite, allowing the production of more lath martensite in the microstructure, which provides higher fracture toughness and higher impact toughness (Ref 25).

Improper Steel Chemistry. Steel hardenability is determined by its chemistry. The quench conditions required to obtain the desired properties are a function of the hardenability. Therefore, if the steel chemistry is incorrect, the selected quench process conditions may, if too severe, lead to cracking. Unfortunately, this problem is not uncommon.

An example of this problem is quench cracking that occurred in AISI 1070 steel bearing raceways. Metallographic analysis confirmed the presence of quench cracking. However, the steel chemistry (Table 6) was incorrect for a plain AISI 1070 steel (Ref 27). The higher-carbon, higher-hardenability steel with a high manganese content, which was found in this example, would be more susceptible to quench cracking, using the normally specified quenchant for the 1070 steel bearing raceways.

Prior Steel Structure. The structure of the steel prior to hardening, for example, extruded, cast, forged, cold formed, and so on, may enhance the potential for cracking during the quench. Each as-formed structure requires a specific time and temperature cycle to condition the material for proper hardening. For example, cast structures must be homogeneous, cold-formed structures require normalization and annealing, and forged structures must be grain-refined by normalization.

Cracking may be caused by microstructures, resulting in nonuniform heating or cooling. In Fig. 31 (Ref 27), microstructures obtained on forged AISI 403 stainless steel valve stems ex-

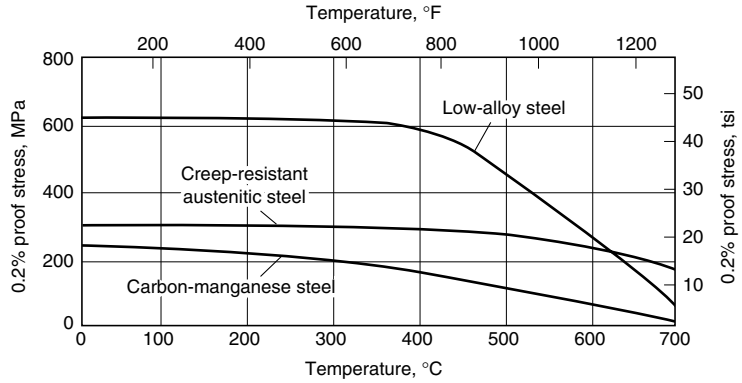

Fig. 20 Variation of yield strength with temperature for three generic classes of steel

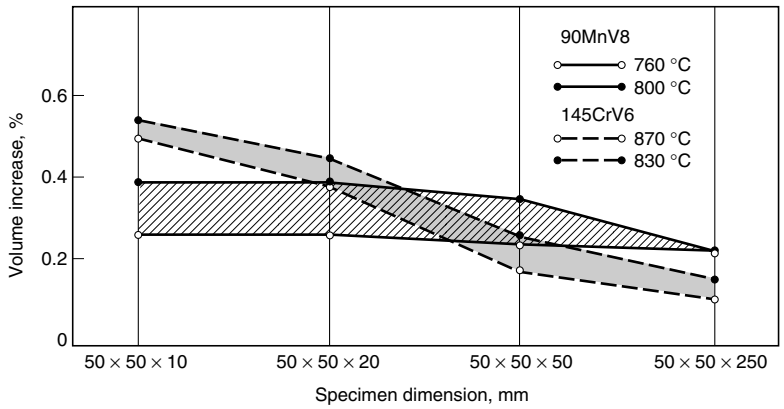

Fig. 21 Volume increase of steels 90MnV8 and 145CrV6 as a function of austenitization temperature and specimen dimensions

hibited longitudinal cracking after quenching. Microstructural analysis suggested that cracking was caused by thermal stresses during forging or during heating prior to forging. Figure 31 also shows a coarse-grain condition associated with high-temperature surface oxidation. Further examination revealed evidence of high- and low-thermal oxidation within the crack profile. The presence of this condition suggests cracking occurred prior to or during forging.

Excessive overheating is called "burning," which refers to incipient melting of low-melting constituents into liquid films that concentrate embrittling components in the grain boundaries, as illustrated in Fig. 32 (Ref 4). The problem of the brittle nature of these films is exacerbated by accompanying void formation, which is caused by contraction shrinkage when the liquid film cools. Although burning usually occurs during rolling or forging, it may not be observed until after heat treatment.

A mixed-grain-size microstructure may be formed when a steel was heated in its coarsening range during austenitization. The hardening response of this mixed microstructure, which is illustrated in Fig. 33, is unpredictable (Ref 4).

When the carbon content of a steel is greater than the eutectoid concentration, it is usually quenched from below the Ac_{cm} temperature (the temperature at which cementite completes solution in austenite), resulting in the presence of undissolved carbides just prior to quenching. This reduces the amount of retained austenite that often accompanies excessive heating temperatures. As is shown subsequently, problems of increased distortion and cracking increase with the retained austenite content. It is important that undissolved carbides be in the dispersed form of spheroids and not in the form of grain-boundary films, which produce a brittle structure after tempering (Ref 4).

The steel austenitizing temperature is a compromise between achieving rapid solution and diffusion of carbon, and minimizing grain growth. A fine-grained steel may be heated to a temperature for rapid austenitization with little danger of grain growth. However, quenched structures formed from large austenite grains exhibit poor toughness and are crack sensitive. The quench cracking illustrated in Fig. 34 occurred because of excessively large austenite grains due to an excessively high austenitizing temperature (Ref 4).

The optimal austenitizing time is determined by dividing the total time in the furnace between heating time (time necessary to bring the part to the austenitizing temperature) and transformation time (the time required to produce the desired microstructural transformation or to complete the desired diffusion process). Excessive heating times to provide for transformation may result in undesirable grain growth.

Heating and Atmosphere Control. Localized overheating is particularly a potential problem for inductively heated parts (Ref 28, 29). Subsequent quenching of the part leads to quench cracks at sharp corners and areas with sudden changes in cross-sectional area (stress raisers). Cracking is due to increases of residual stresses at the stress raisers during the quenching process. The solution to the problem is to increase the heating speed by increasing the power density of the inductor. The temperature difference across the heated zone is decreased by continuous heating or scanning of several pistons together on a single bar (Ref 29).

For heat treating problems related to furnace design and operation, it is usually suggested that (Ref 28):

- The vestibules of atmosphere-hardening furnaces should be loaded and unloaded with purging. Load transfer for belt and shaker hearth furnaces should only occur with thorough purging to minimize atmosphere contamination.
- Hardening furnaces typically contain excessive loads prior to quenching. If the steel at quenching temperature is greater than 20% of

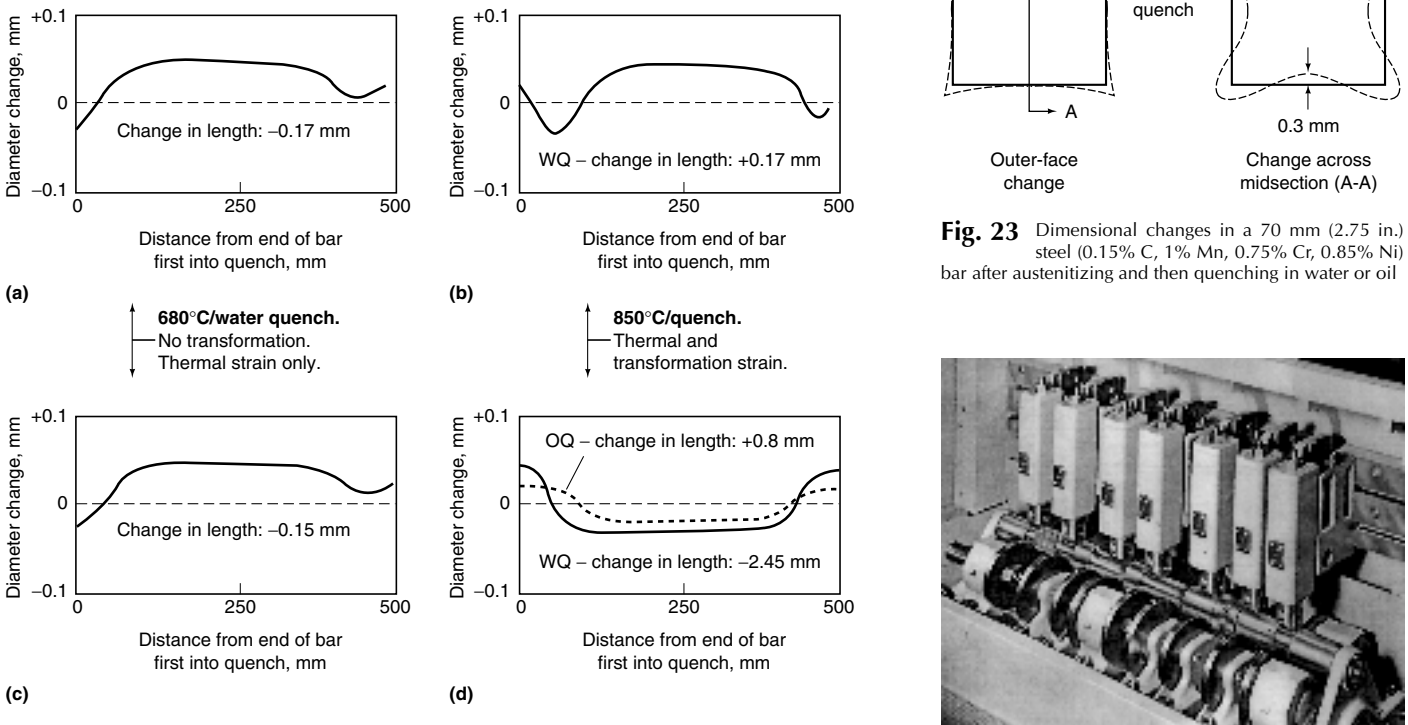

Fig. 22 Dimensional variation of a medium-carbon (0.4%) steel bar (200 mm, or 8 in., diam × 500 mm, or 20 in.) after the indicated heat treatments. These bars were quenched vertically with one end down (marked "0" in the figure). (a) and (c) show no transformation, thermal strain only after water quenching from 680 °C (1260 °F). (b) and (d) show thermal and transformation strains after quenching from 850 °C (1560 °C). OQ, oil quench; WQ, water quench

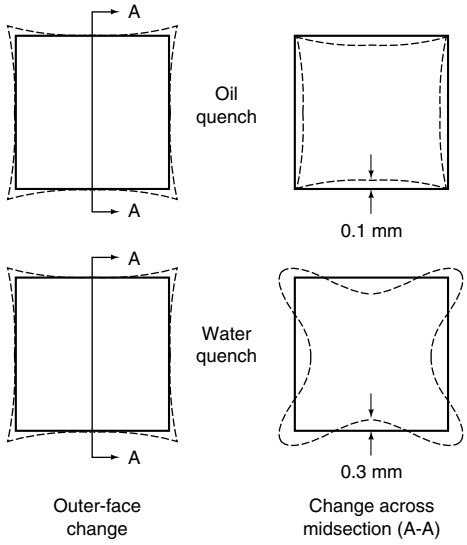

Fig. 23 Dimensional changes in a 70 mm (2.75 in.) steel (0.15% C, 1% Mn, 0.75% Cr, 0.85% Ni) bar after austenitizing and then quenching in water or oil

Fig. 24 Die quenching system. Courtesy of Gleason Tooling Products Group

the distance from discharge to charge door, it is too much. Either the production rate can be increased or some of the burners can be turned off.

One source of cracking, which may appear similar to quench cracking, can also occur due to excessive heating rate to the austenitizing temperature. This is illustrated for AISI 4140 steel in Fig. 35 (Ref 27). In this case, surface oxidation and decarburization within the crack, which would not have been obtained if the cracking occurred during the quench, was observed.

Cracking may also be due to localized overheating (nonuniform heating), shown in Fig. 36, which is a microstructure of AISI 4140 tube end sections (Ref 27). Circumferential cracking at a mid-thickness location of the sample was reported on the tube end. The tubes were reportedly austenitized and then spray quenched. Microstructural examination of the steel revealed a coarse-grain condition due to overheating during austenitization prior to quenching. The cracking occurred along the coarse-grain boundary, as illustrated in Fig. 36. However, microstructural analysis of samples from other regions of the tube indicated fine-grain martensite. Taken together, these data suggest that the austenitization furnace contained hot spots that caused localized overheating and grain coarsening. The overheated locations cracked in the presence of quench stresses. Cracking occurred in the mid-thickness locations due to the inherent weakness of the material centers carried over from the original billet or casting.

An important source of steel distortion and cracking is nonuniform heating and not using the appropriate protective atmosphere. For example, if steel is heated in a direct-gas-fired furnace with high moisture content, the load being heated may adsorb hydrogen, leading to hydrogen embrittlement and subsequent cracking, which would not normally occur with a dry atmosphere (Ref 22, 28).

Component Support and Loading. Many parts may sag and creep under their own weight when heat treated, which is an important cause of distortion. An example of a type of component that is susceptible to such distortion is a ring gear. The dimension limits by which ring gears are classified are provided in Fig. 37 (Ref 21). (A general dimensional classification of various distortion-sensitive shapes is provided in Fig. 38 [Ref 21].) Proper support when heating is required to minimize out-of-flatness and ovality problems, which may result in long grinding times, excessive stock removal, high scrap losses, and loss of case depth (Ref 21). To achieve adequate distortion control, custom supports or press quenching may be required.

Pinion shafts, as defined in Fig. 39, are susceptible to banding along their length, if they are improperly loaded into the furnace, as shown in Fig. 40 (Ref 21). When this occurs, the pinion shafts must then be straightened, which adds to production cost.

Surface Condition. Quench cracking may be due to various steel-related problems that are only observable after the quench, but the root cause is not the quenching process itself. These prior conditions include prior steel structure, stress raisers from prior machining, laps and seams, alloy inclusion defects, grinding cracks, chemical segregation (bonding), and alloy depletion (Ref 27).

One prior-condition problem is tight scale, which is encountered with forgings hardened from direct-fired gas furnaces with high-pressure burners (Ref 23, 24). The effect of tight scale on the quenching properties of two steels, 1095 carbon steel and 18-8 stainless steel, is illustrated in Fig. 41 (Ref 25). These cooling curves were obtained by still quenching into fast oil. A scale of not more than 0.08 mm (0.003 in.) increases the rate of cooling of 1095 steel as compared to the rate obtained on a specimen without scale. However, a heavy scale (0.13 mm, or 0.005 in.)

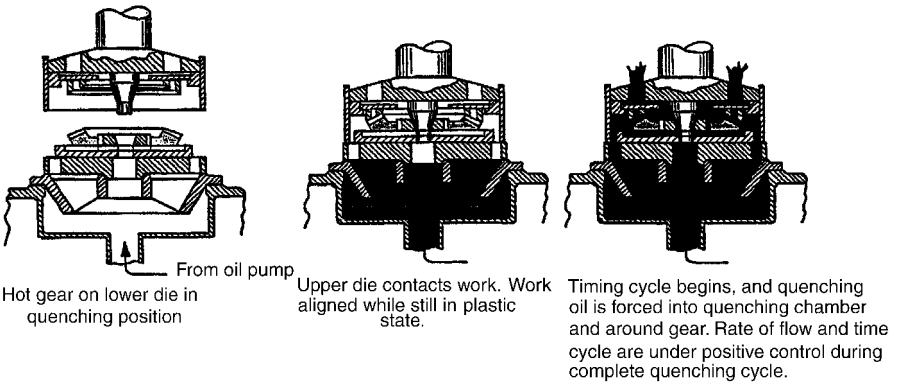

Fig. 25 Schematic of a press quench system. Courtesy of Gleason Tooling Products Group

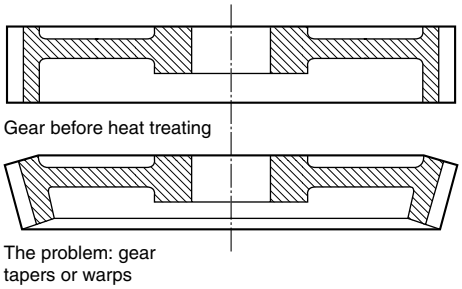

Fig. 26 Schematic of a gear that is difficult to harden without the distortion shown

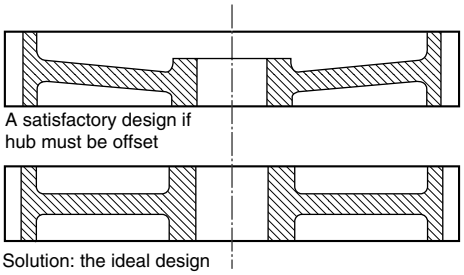

Fig. 27 Design solutions to the distortion problem shown in Fig. 26

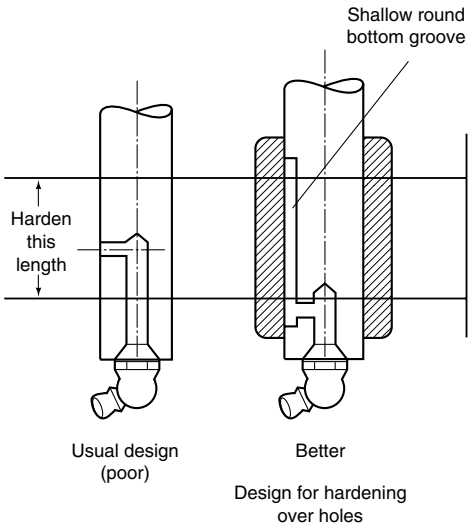

Fig. 28 Design solutions to the quench-cracking problem often encountered in shaft hardening over a cross hole

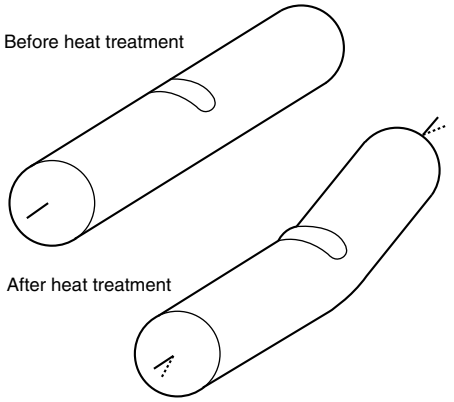

Fig. 29 Distortion often encountered when quenching a notch

deep retards the cooling rate. A very light scale, 0.013 mm (0.0005 in.) deep, also increased the cooling rate of the 18-8 steel over that obtained with the specimen without scale.

In practice, the formation of tight scale varies in depth over the surface of the part, resulting in thermal gradients due to differences in cooling rates. This problem may yield soft spots and uncontrolled distortion and is particularly a problem with nickel-containing steels. Surface oxide formation can be minimized by the use of an appropriate protective atmosphere.

The second surface-related condition is decarburization, which may lead to increased distortion or cracking (Ref 26). At a given depth within the decarburized layer, the part does not harden as completely as it would at the same point below the surface if there were no decarburization. This leads to nonuniform hardness, which may contribute to increased distortion and cracking, because (Ref 23):

- The decarburized surface transforms at a higher temperature than the core (the M_s temperature decreases with carbon content). This leads to high residual tensile stresses at the decarburized surface or a condition of unbalanced stresses and distortion.
- Because the surface is decarburized, it exhibits lower hardenability than the core. This causes the upper transformation products to form early, nucleating additional undesirable products in the core. The decarburized side is softer than the side that did not undergo decarburizing, which is harder. The greater amount of martensite leads to distortion.

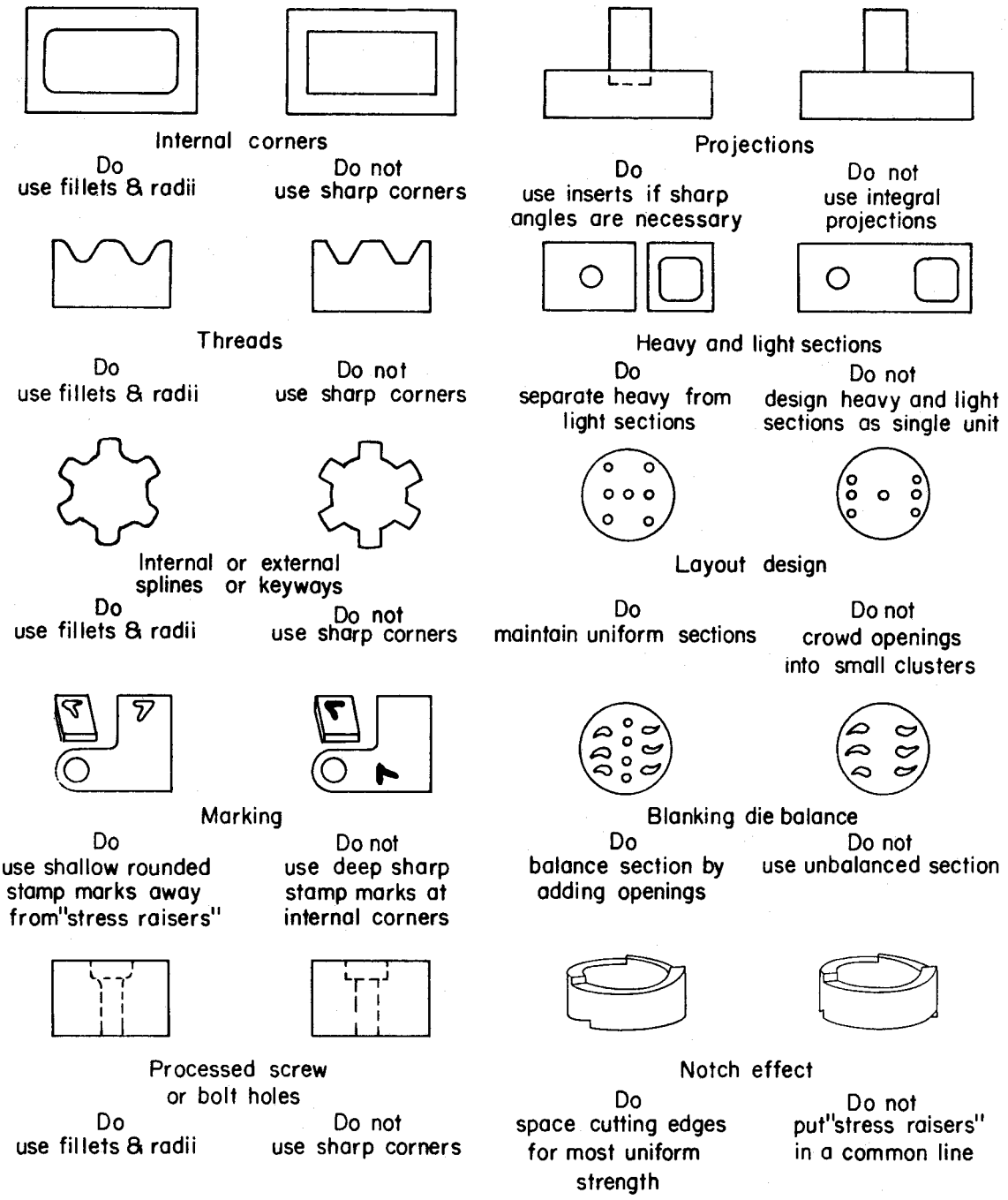

Fig. 30 Part design recommendations for minimal internal stresses. Source: Ref 4

The solution to this problem is to restore carbon into the furnace atmosphere or to remove the decarburized layer by machining.

Another surface-related condition that may lead to cracking or material weakening is the formation of surface seams or nonmetallic inclusions, which may occur in hot-rolled or cold-finished material. The presence of these defects prevents the hot steel from welding to itself during the forging process, for example, creating a stress raiser. To prevent this problem with hot-rolled bars, stock should be removed before heat treatment. Recommendations are provided in Table 7 (Ref 24).

A seam or nonmetallic depth of 0.025 mm (0.001 in.) per 3.3 mm (0.13 in.) diameter maximum is usually acceptable for cold-finished bars (Ref 24). If the seam depth is excessive, it is recommended that the bars be magnaflux inspected prior to heat treatment.

Stress Raisers from Prior Machining, Laps, and Seams. Surface conditions from prior machining conditions act as stress raisers, which are areas of dimensional changes (Fig. 42) (Ref 27). Examples of such stress raisers include fillets (Fig. 43), thread and gear roots and machining marks (Fig. 44 and 45 respectively), rolling seams (Fig. 46 and 47), and forging laps (Fig. 48 and 49). Forging laps are due to concentrations of oxides that are folded in during the forging process. The presence of these oxides prevents the hot steel from welding to itself during the forging process. This leads to cracking, as shown. (Note: The sample is first viewed in the

Table 5 Suggested carbon-content limits for water, brine, and caustic quenching

Shapes	Maximum carbon content, %
Furnace hardening	
General use	0.30
Simple shapes	0.35
Very simple shapes (e.g., bars)	0.40
Induction hardening	
Simple shapes	0.50
Complex shapes	0.33

Table 6 Comparison of steel obtained and specification range of steel chemistry of AISI 1070 steel used for bearing raceway problem

Element	Specification range for AISI 1070, %	Content in steel obtained, %
Carbon	0.65–0.75	0.74
Manganese	0.60–0.90	0.97
Phosphorus	0.11	0.04
Sulfur	0.026	0.05
Silicon	0.10–0.20	0.23
Nickel	. . .	0.07
Chromium	. . .	0.11
Molybdenum	. . .	0.22
Copper	. . .	0.10

Fig. 31 Micrograph of type 403 stainless steel as-forged. The microstructure is predominantly a mixture of carbide particles in a matrix of ferrite. No evidence of quenching and tempering was observed. High- and low-temperature oxidation can be observed on the surface of the sample and within the crack profile. 100×; Villela's reagent. Source: Ref 27

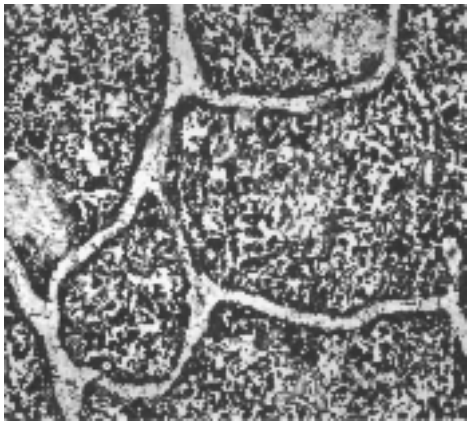

Fig. 32 Severely overheated 1038 steel showing initial stage of burning. Ferrite (white) outlines prior coarse austenite grain boundaries; matrix consists of ferrite (white) and pearlite (black). Source: Ref 4

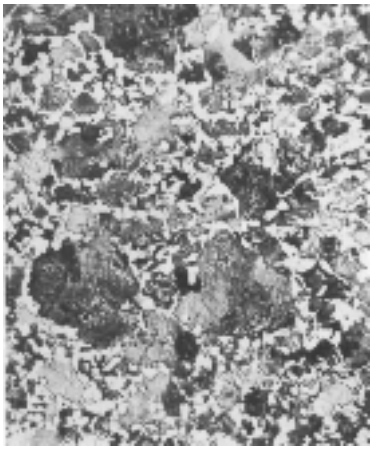

Fig. 33 AISI 1040 steel bar austenitized at 913 °C (1675 °F) for 30 min, then cooled slowly in a furnace. White areas are ferrite; dark areas are pearlite. Mixed grain size due to heating into the coarsening range is also observed. Source: Ref 4

Fig. 34 Quench cracks due to excessively large grain boundaries resulting from excessively high austenitizing temperature. Note cracking patterns associated with prior coarse austenite grain boundaries. Source: Ref 4

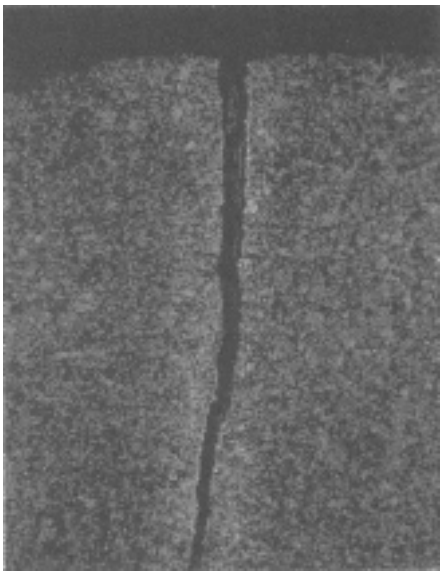

Fig. 35 Micrograph of AISI 4140 steel as quenched and tempered. The microstructure is tempered martensite with evidence of decarburization and high-temperature oxidation on the surface of the crack profile. 50×; 2% nital etch. Source: Ref 27

unetched condition to locate the crack. Then, the sample is etched, if desired, for microstructural identification.)

Several types of internal voids may be present in steel. The first type is known as a pipe void, which is an imperfection formed after casting and cooling (see the article "Failures Related to Metal Working and Machining Operations", in this volume). The pipe void is a cavity formed by contraction during solidification of the last portion of liquid metal in the ingot and may even survive rolling or forging, but, because the ends of the ingot are closed, it is not detected until the bar stock is cut, at which time it is readily visible.

Another type of internal void is a forge or roll burst. The pipe void is readily distinguishable from the forge or roll burst by the more rounded nature of the pipe void compared to the thin, cracklike appearance of the forge or roll burst. Steel porosity also produces voids in steel castings. These voids are caused by trapped gases. Porosity is another source of potential steel cracking. This is illustrated in Fig. 50 (Ref 27).

Nonmetallic Inclusions. All steels contain numerous nonmetallic inclusions, but the cleaner grades have fewer large or significant inclusions than do the conventional grades. There are two types of nonmetallic inclusions. Exogenous nonmetallic inclusions occur when particles or large lumps of refractory fall into the molten steel during the steelmaking process. These contaminants provide surfaces in which indigenous inclusions may nucleate and grow. Indigenous inclusions arise from reactions, such as deoxidation products Al_2O_3 and SiO_2 or desulfurization products such as MnS (Ref 30).

Nonmetallic inclusions may exhibit degraded transverse toughness and ductility. They may also reduce fatigue strength, although soft inclusions are less harmful than are hard inclusions of the same size. In carburized parts, although nonmetallic inclusions may not significantly affect the fatigue limit, they could result. Figure 51 illustrates a combination of nonmetallic inclusions and banding due to microsegregation (discussed subsequently) (Ref 30). If a void is present at the site of a nonmetallic inclusion, possibly due to forging, the degree that the defect acts as a stress raiser increases. However, by some mechanism, such as shearing, the stress-raising effect may decrease, as illustrated by Fig. 52, where the nonmetallic inclusion appears as a "butterfly" after etching (Ref 30).

Machining. Material removal during machining can result in high residual stress levels and, ultimately, unacceptable distortion (Ref 21). When excessive machining stresses are imparted, the process may require modification to include a rough machining stress relieving followed by fine machining. Tables 8 and 9 are the suggested AISI design minimum allowable tolerances for machining (Ref 4).

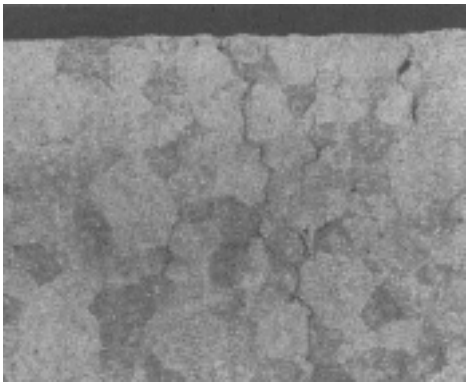

Fig. 36 Micrograph of AISI 4140 steel as quenched and tempered. The microstructure is tempered martensite with intergranular quench cracking along the prior austenite grain boundaries. 100×; 2% nital etch. Source: Ref 27

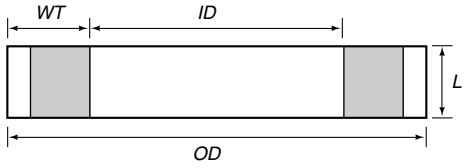

Fig. 37 Dimensions of a ring gear shape. Shape limitation: length/wall thickness ≤ 1.5; inside diameter (ID)/outside diameter (OD) > 0.4. Minimum wall thickness (WT) is defined by WT ≥ 2.25 × module + [0.4 × 5 (mod × L × $OD^3)^{1/2}$]

Quenching

Quenchant Selection and Severity

Quenchants must be selected to provide cooling rates capable of producing acceptable microstructure in the section thickness of interest. However, it is not desirable to use quenchants with excessively high heat-removal rates. Typically, the greater the quench severity, the greater the propensity to increased distortion or crack-

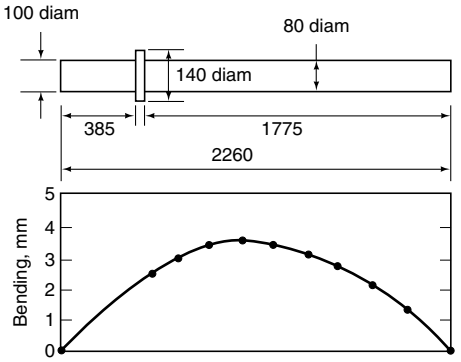

Fig. 39 Distortion of JIS SCM 440 (0.4% C, 1.05% Cr, 0.22% Mo) steel pinion shafts after oil quenching from 850 °C (1560 °F) while vertically suspended and tempering at 600 °C (1110 °F)

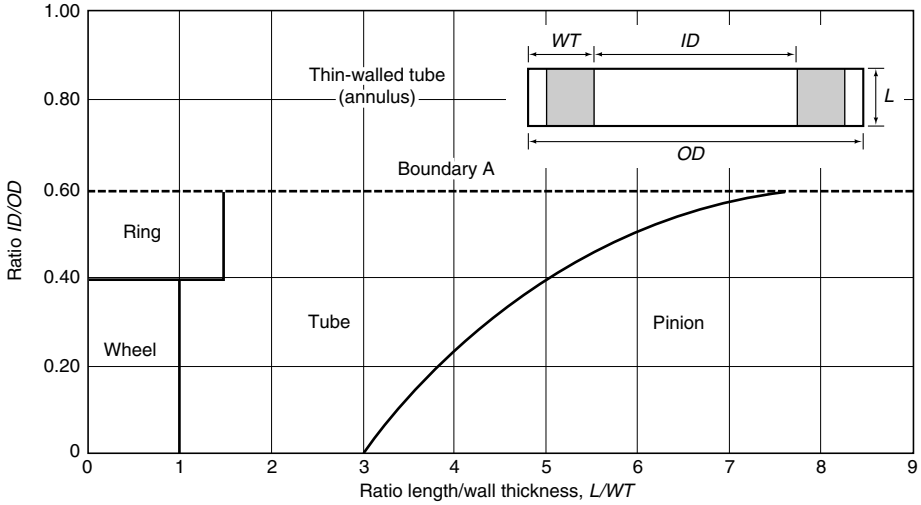

Fig. 38 Classification of distortion-sensitive shapes

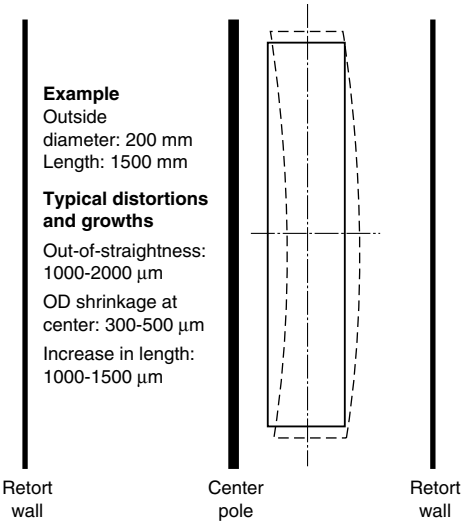

Fig. 40 Example of pinion shaft distortion due to furnace loading

ing. Although a reduction of quench severity leads to reduced distortion, it may also be accompanied by undesirable microstructures. Therefore, it is difficult to select an optimal quenchant and agitation. Cooling power (quench severity) of quenchant should be as low as possible while maintaining a sufficiently high cooling rate to ensure the required microstructure, hardness, and strength in critical sections of the steel parts.

Quench severity is defined as the "ability of a quenching medium to extract heat from a hot steel workpiece, expressed in terms of the Grossmann number (*H*)" (Ref 31). A typical range of Grossmann *H*-values (numbers) for commonly used quench media are provided in Table 10, and Fig. 53 provides a correlation between the *H*-value and the ability to harden steel, as indicated by the Jominy distance (*J*-distance) (Ref 23). Although Table 10 is useful to obtain a relative measure of the quench severity offered by different quench media, it is difficult to apply in practice, because the actual flow rates for "moderate," "good," "strong," and "violent" agitation are unknown.

Alternatively, the measurement of actual cooling rates or heat fluxes provided by a specific quenching medium does provide a quantitative meaning to the quench severity provided. Some illustrative values are provided in Table 11 (Ref 32).

Typically, the greater the quench severity, the greater the propensity of a given quenching medium to cause distortion or cracking. This usually is the result of increased thermal stress, not transformational stresses. Specific recommendations for quench media selection for use with

Table 7 Minimum recommended material removal from hot-rolled steel products to prevent surface seam and nonmetallic stringer problems during heat treatment

	Minimum material removal per side(a)	
Condition	**Nonresulfurized**	**Resulfurized**
Turned on centers	3% of diameter	3.8% of diameter
Centerless turned or ground	2.6%	3.4%

(a) Based on bars purchased to special straightness, i.e., 3.3 mm (0.13 in.) in 1.5 m (5 ft) maximum

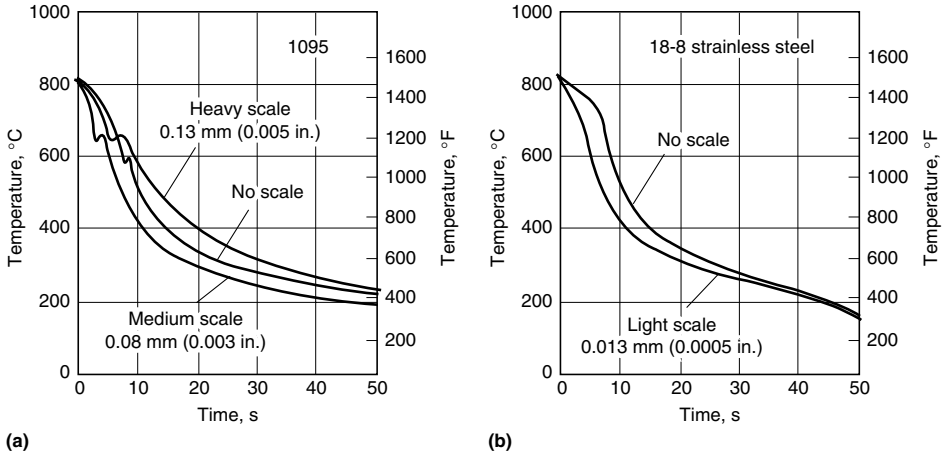

Fig. 41 Centerline cooling curves showing the effect of scale on the cooling curves of two different steels quenched in fast oil without agitation. (a) 1095 steel; oil temperature, 50 °C (125 °F). (b) 18-8 stainless steel; oil temperature, 25 °C (75 °F). Test specimens were 13 mm (0.5 in.) diam by 64 mm (2.5 in.) long

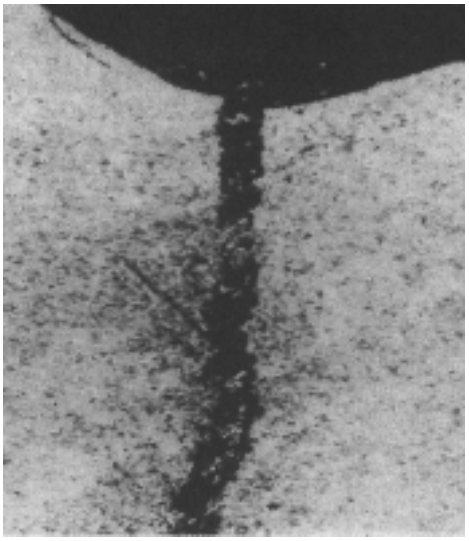

Fig. 44 Micrograph of AISI 4140 steel as quenched and tempered. The microstructure is tempered martensite with quench cracking initiating from a machine groove. 100×; 2% nital etch. Source: Ref 27

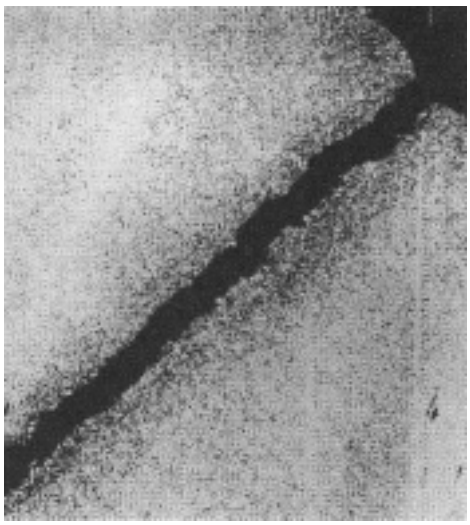

Fig. 42 Micrograph of AISI 4140 steel as quenched and tempered. The microstructure is tempered martensite with quench cracking in the area of dimensional change. 91×; 2% nital etch. Source: Ref 27

Fig. 43 Micrograph of AISI 4142 steel as quenched and tempered. The microstructure is tempered martensite with quench cracking at the fillet radius. 100×; 3% nital etch. Source: Ref 27

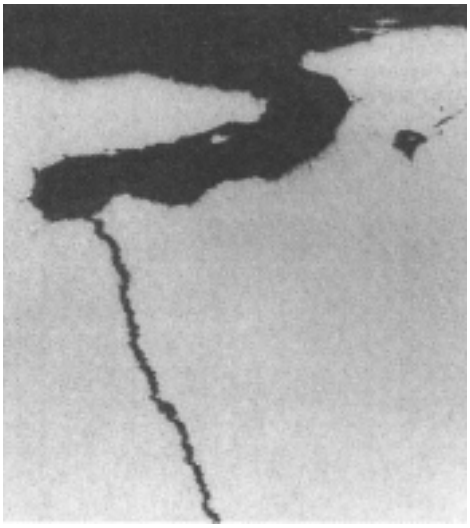

Fig. 45 Micrograph of AISI 4118 carburized steel as quenched and tempered. The microstructure is tempered martensite (unetched) with a quench crack propagating from a machining burr. 200×. Source: Ref 27

various steel alloys is provided by standards such as Aerospace Material Specification (AMS) 2759. Figure 54 illustrates a quench crack due to an excessively high cooling rate (Ref 27).

Some additional general comments regarding quenchant selection include (Ref 23, 28):

- Most machined parts made from alloy steels are oil quenched to minimize distortion. Most small parts or finish-ground larger parts are "free" quenched. Larger gears, typically those greater than 20 cm (8 in.), are fixture (die) quenched to control distortion. Smaller gears and parts, such as bushings, are typically plug quenched on a splined plug, which is usually constructed from carburized 8620 steel.
- Although a reduction of quench severity leads to reduced distortion, it may also be accompanied by undesirable microstructures, such as the formation of upper bainite (quenched pearlite) with carburized parts.
- Quench speed may be reduced by quenching in hot (570 to 750 °C, or 1060 to 1380 °F) oil. When hot oil quenching is used for carburized steels, lower bainite, which exhibits properties similar to martensite, is formed.
- Excellent distortion is typically obtained with austempering, quenching into a medium just above the M_s temperature. The formation of retained austenite is a significant problem with austempering processes. Retained austenite is most pronounced where manganese and nickel are major components. The best steels for austempering are plain carbon steels and chromium and molybdenum alloy steels (Ref 23).
- Aqueous polymer quenchants may often be used to replace quench oils, but quench severity is still of primary importance and appropriate quench system design is necessary.
- Gas or air quenching provides the least distortion and may be used if the steel has sufficient hardenability to provide the desired properties.
- Low-hardenability steels are quenched in brine or vigorously agitated oil. However, even with a severe quench, undesirable microstructures, such as ferrite, pearlite, or bainite, can form.

Fig. 46 Micrograph of AISI 8630 steel as quenched. The microstructure is martensite, where cracking initiated from a rolling seam. Source: Ref 27

Fig. 47 Micrograph of type 403 stainless steel as quenched and tempered. The microstructure is predominantly tempered martensite, with cracking promoted by the seam. 100×; Vilella's reagent. Source: Ref 27

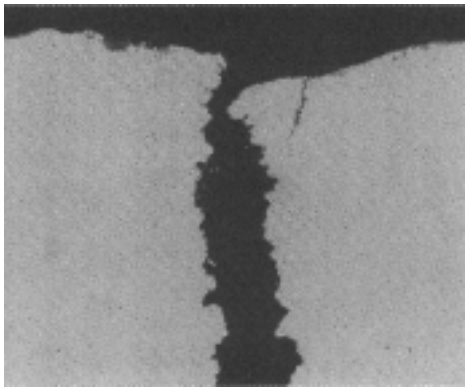

Fig. 48 Micrograph of AISI 1030 steel as direct-forge quenched and tempered. The microstructure is tempered martensite (unetched) with forged-in scale adjacent to cracking. 100×. Source: Ref 27

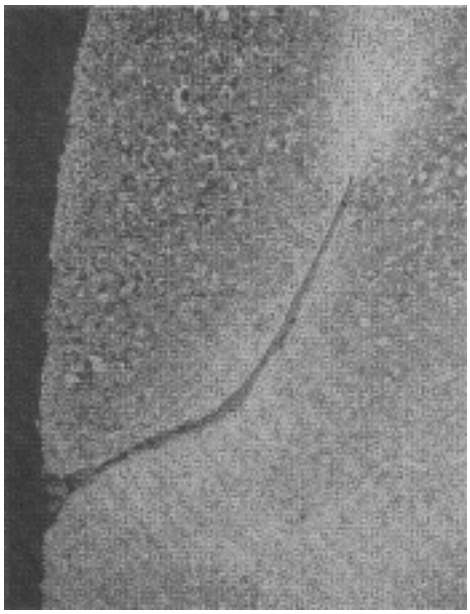

Fig. 49 Micrograph of AISI 1045 as-forged steel illustrating a forging lap. 27×; 2% nital etch. Source: Ref 27

Quenchant Uniformity

Quench nonuniformity is one of the greatest contributors to quench cracking. Quench nonuniformity can arise from nonuniform flow fields

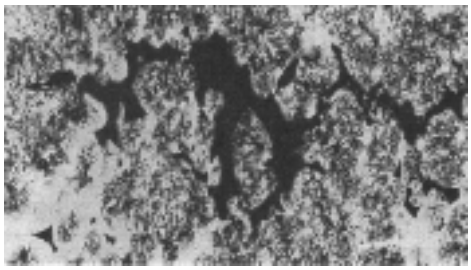

Fig. 50 Micrograph of AISI 8630 cast steel as quenched and tempered. The microstructure is tempered martensite, pearlite, and ferrite, showing a potential cracking condition. 91×; 3% nital etch. Source: Ref 27

Fig. 51 Nonmetallic inclusions and banding in a microsegrated 1% C alloy steel showing retained austenite. Source: Ref 30

around the part surface during the quench or non-uniform wetting of the surface (Ref 23, 33–35). Both lead to nonuniform heat transfer during quenching. Nonuniform quenching creates large thermal gradients between the core and the surface of the part. The effect of nonuniform quenching is illustrated with forged AISI 1045 crankshafts in Fig. 55 and 56 (Ref 27). Microstructural examination showed a mixture of nonuniform cross-sectional microstructures. Areas of tempered martensite adjacent to pearlite, bainite, acicular ferrite, and ferrite at prior austenite grain boundaries were observed.

Poor agitation design is a major source of quench nonuniformity. The purpose of the agitation system is not only to take hot fluid away from the surface and to the heat exchanger, but it is also to provide uniform heat removal over the entire cooling surface of all of the parts throughout the load being quenched. The batch quench system in Fig. 57 illustrates a system where axial (vertical) quenchant flow occurs throughout a load of round bars lying horizontally in a basket (Ref 22). In this case, the bottom surfaces of the bars experience greater agitation than the top surfaces. Cracks form on the upper surfaces because of the nonuniform heat loss. Agitation produces greater heat loss at the bottom, creating a large thermal gradient between the top and the bottom surfaces.

If a submerged spray manifold is used to facilitate more uniform heat removal, the following design guidelines are recommended:

- The total surface of the part should experience uniform quenchant impingement.
- The largest holes possible (2.3 mm, or 0.09 in., minimum) should be used.
- The manifold face should be at least 13 mm (0.5 in.) from the surface of the parts being quenched.
- Repeated removal of hot quenchant and vapor should be possible.

Excessive distortion was also obtained with an agitation system, illustrated in Fig. 58, when the quenchant flow was either in the same direction relative to the direction of part immersion or in the opposite direction (Ref 35). The solution to this problem was to minimize the quenchant flow to that required for adequate heat transfer during the quench and to provide agitation by mechanically moving the part up and down in the quenchant. Identifying sources of nonuniform fluid flow during quenching continues to be an important tool for optimizing distortion control and minimizing quench cracking.

Nonuniform thermal gradients during quenching are also related to interfacial wetting kinematics, which is of particular interest with vaporizable liquid quenchants, including water, oil, and aqueous polymer solutions (Ref 36). Most liquid vaporizable quenchants exhibit boiling temperatures between 100 and 300 °C (210 and 570 °F) at atmospheric pressure. When parts are quenched in these fluids, surface wetting is usually time-dependent, which influences the cooling process and the achievable hardness.

Another major source of nonuniform quenching is foaming and contamination. Contaminants include sludge, carbon, and other insoluble materials. It includes water in oil, oil in water, and aqueous polymer quenchants. Foaming and contamination leads to soft spotting, increased distortion, and cracking.

Quench Distortion and Cracking

In the previous discussion, two quenchant-related phenomenon have been discussed: quench cracking and quench distortion. Although quench cracking can be eliminated, quench distortion cannot. Instead, the issue is distortion control, not elimination. Both quenching-related distortion control and quench cracking are discussed here.

Quench Distortion. One form of distortion that may occur on quenching is defined as shape distortion, which is dimensional variation that occurs when the parts are hot and the stress of their own weight leads to dimensional variation, such as bending, warpage, and twisting (Ref 34). Shape distortion is attributable to component support and loading, as discussed previously.

A second form of distortion is size distortion, which includes dimensional changes observable as elongation, shrinkage, thickening, and thinning. Size distortion is due to the volumetric variation that accompanies each of the transformational phases formed on quenching (Ref 34). Size distortion can be further classified as one-dimensional, two-dimensional, and three-dimensional. One-dimensional distortion is exemplified by the change in length when rods or wire are quenched and is primarily due to transformational distortion. Two-dimensional distortion is also primarily due to transformational distortion, and it is exemplified by size variation in two dimensions, such as would occur with sheet or plate stock on quenching. With bulk material that can undergo dimensional variation in three dimensions, the problem is due to both thermal and transformational distortion and is much more complicated (Ref 34). It has been shown that one of the primary contributors to quench distortion is uneven (nonuniform) cooling.

Quench Cracking. One major source of steel cracking is excessive cooling rates during the quench (quench severity). This is illustrated in Fig. 54 (Ref 27). Note that the crack passes straight from the surface to the core. Excessive cooling rates (high quench severity) produce greater thermal stresses in addition to greater transformation stresses. Steel cracking during transformation to martensite is largely due to the volumetric increase that accompanies martensite formation. If the total residual stresses in the part are sufficiently high, quench cracking occurs.

Although quench distortion and cracking are most often due to nonuniform cooling, materials selection can be an important factor. The following materials selection rules are helpful:

- The compositional tolerances should be checked to ensure that the alloy is within specification.
- It is often better to choose a lower carbon content, because the higher carbon content often causes higher susceptibility for distortion and cracking.
- If possible, it is better to choose a combination of high-alloy steel and very slow cooling. As a matter of course, the selection of high-alloy steels markedly raises the material cost.

Cracking tendency decreases as the start of the martensitic transformation temperature (M_s) increases (Ref 37). Kunitake and Susigawa developed a relationship to interrelate the combined effect of both carbon content and elemental composition on the cracking propensity of steel. This was designated as the carbon equivalent (CE); the equation for calculating this value is provided in Fig. 59, where it is seen that quench cracks are prevalent at CE values above 0.525 (Ref 37).

Stresses that lead to cracking are thermal and often nonuniform cooling from T_A and M_s and transformational stress formed between M_s and

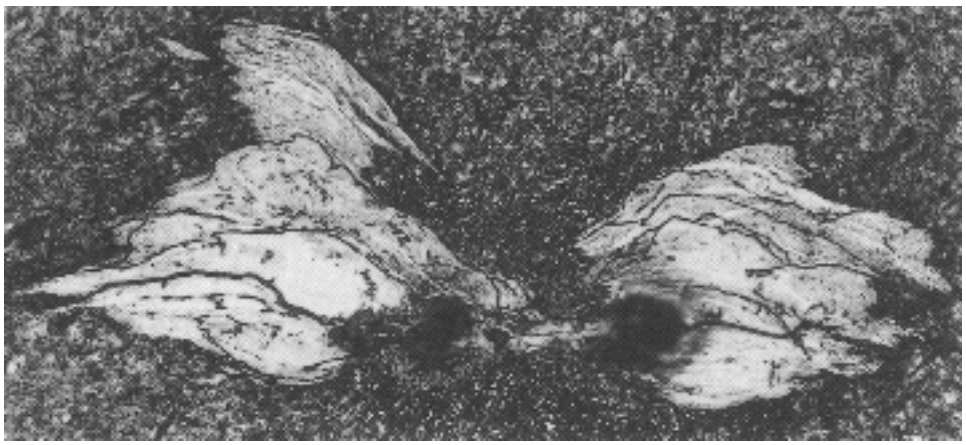

Fig. 52 White "butterfly" etching developed at a nonmetallic inclusion as a result of contact loading. 675×. Source: Ref 30

martensite finish temperature (M_f). Nonuniform thermal stresses occur when nonuniform surface cooling occurs. In this case, there is a deferred contraction in the slower cooling areas, creating a pull stress resulting in pull cracking (Ref 36). This is illustrated in Fig. 60(a) (Ref 36), where rapid but nonuniform surface cooling to point A has occurred, at which time it affects adjacent point B, which is cooling more slowly, causing a deferred contraction at point B′—both of which occur while the martensitic transformation occurs at the M_s point. As a result, point A, which cooled rapidly, undergoes compression, and point B′, which cooled more slowly, undergoes pulling. This means that pull stress is a tensile stress, and if this stress becomes large enough, cracking occurs in areas where cooling is delayed.

When there is nonuniform cooling within the part between the M_s and M_f, there is a stretching or elongation in areas where the cooling is slow, which acts as a push stress, leading to push cracking (Ref 38). This is illustrated by Fig. 60(b) (Ref 36), where point A, which cooled rapidly, stretches point B (which cooled more slowly) to point B′ below the M_s temperature, which is a state that undergoes the expansion due to martensitic transformation. As a result, the rapidly cooled point A (exterior) undergoes pulling, and the slowly cooled point B′ (interior) undergoes compression. This results in interior point B′ causing pushing and cracking at point A, which occurs in areas where quenching occurs rapidly.

Therefore, pull cracking, which occurs with nonuniform surface cooling between T_A and M_s, and push cracking, which occurs with nonuniform cooling within the part between M_s and M_f, are the opposite of each other, although the cracking event takes place for both between the M_s and M_f. Figure 61 provides illustrations of both push and pull cracking (Ref 36).

For cracking to occur, the presence of a stress raiser (points of stress concentration) is typically necessary. Two types of stress raisers may be

Table 8 Minimum allowance for machining flat and square bars

Specified thickness, in., incl(a)		Specified width, in., incl										
		0 to ½	Over ½ to 1	Over 1 to 2	Over 2 to 3	Over 3 to 4	Over 4 to 5	Over 5 to 6	Over 6 to 7	Over 7 to 8	Over 8 to 9	Over 9 to 12
Hot-rolled square and flat bars												
0 to ½	A	0.025	0.025	0.030	0.035	0.040	0.045	0.050	0.055	0.060	0.060	0.060
	B	0.025	0.035	0.040	0.050	0.065	0.080	0.095	0.105	0.120	0.130	0.140
Over ½ to 1	A	. . .	0.045	0.045	0.050	0.055	0.060	0.065	0.070	0.075	0.075	0.075
	B	. . .	0.045	0.050	0.060	0.075	0.095	0.115	0.130	0.150	0.155	0.155
Over 1 to 2	A	. . .	. . .	0.065	0.065	0.070	0.070	0.075	0.080	0.080	0.095	0100
	B	. . .	. . .	0.065	0.070	0.085	0.105	0.125	0.145	0.165	0.170	0.170
Over 2 to 3	A	. . .	. . .	. . .	0.085	0.085	0.085	0.085	0.090	0.100	0.100	0.100
	B	. . .	. . .	. . .	0.085	0.100	0.120	0.135	0.155	0.170	0.190	0.190
Over 3 to 4	A	. . .	. . .	. . .	. . .	0.115	0.115	0.115	0.115	0.125	0.125	0.125
	B	. . .	. . .	. . .	. . .	0.115	0.125	0.140	0.170	0.190	0.190	0.190
Cold-drawn square and flat bars												
0 to ½	A	0.025	0.025	0.030	0.035	0.040	0.045	. . .	. . .	. . .	. . .	. . .
	B	0.025	0.035	0.040	0.050	0.065	0.080	. . .	. . .	. . .	. . .	. . .
Over ½ to 1	A	. . .	0.045	0.045	0.050	0.055	0.060	. . .	. . .	. . .	. . .	. . .
	B	. . .	0.045	0.050	0.060	0.075	0.095	. . .	. . .	. . .	. . .	. . .
Over 1 to 2	A	. . .	. . .	0.065	0.065	0.070	. . .	. . .	. . .	. . .	. . .	. . .
	B	. . .	. . .	0.065	0.070	0.085	. . .	. . .	. . .	. . .	. . .	. . .
Forged square and flat bars												
Over ½ to 1	A	. . .	. . .	0.060	0.065	0.065	0.075	0.080	0.085	0.090	0.100	0.110
	B	. . .	. . .	0.072	0.084	0.100	0.120	0.144	0.168	0.200	0.200	0.200
Over 1 to 2	A	. . .	. . .	0.090	0.090	0.090	0.100	0.110	0.115	0.125	0.140	0.150
	B	. . .	. . .	0.090	0.100	0.108	0.124	0.148	0.172	0.200	0.200	0.200
Over 2 to 3	A	. . .	. . .	. . .	0.120	0.120	0.125	0.130	0.135	0.150	0.160	0.175
	B	. . .	. . .	. . .	0.120	0.136	0.140	0.148	0.172	0.200	0.200	0.200
Over 3 to 4	A	. . .	. . .	. . .	. . .	0.150	0.150	0.160	0.180	0.200	0.210	0.225
	B	. . .	. . .	. . .	. . .	0150	0.150	0.160	0.180	0.200	0.210	0.225
Over 4 to 5	A	. . .	. . .	. . .	. . .	. . .	0.180	0.180	0.190	0.210	0.225	0.250
	B	. . .	. . .	. . .	. . .	. . .	0.180	0.180	0.190	0.210	0.225	0.250
Over 5 to 6	A	. . .	. . .	. . .	. . .	. . .	. . .	0.210	0.225	0.125	0.250	0.250
	B	. . .	. . .	. . .	. . .	. . .	. . .	0.210	0.225	0.225	0.250	0.250
Over 6 to 7	A	. . .	. . .	. . .	. . .	. . .	. . .	. . .	0.250	0.250	0.250	0.250
	B	. . .	. . .	. . .	. . .	. . .	. . .	. . .	0.250	0.250	0.250	0.250

(a) Minimum allowance, inches per side, for machining prior to heat treatment. A, allowance on thickness, in. per side; B, allowance on width, in. per side

Table 9 Minimum allowance per side for machining rounds, hexagons, and octagons prior to heat treatment

Ordered size, in., incl	Minimum allowance per side, in.			
	Hot rolled	Forged	Rounds rough turned	Cold drawn
Up to ½	0.016	. . .	. . .	0.016
Over ½ to 1	0.031	. . .	. . .	0.031
Over 1 to 2	0.048	0.072	. . .	0.048
Over 2 to 3	0.063	0.094	0.020	0.063
Over 3 to 4	0.088	0.120	0.024	0.088
Over 4 to 5	0.112	0.145	0.032	. . .
Over 5 to 6	0.150	0.170	0.040	. . .
Over 6 to 8	0.200	0.200	0.048	. . .
Over 8 to 10	0.200	0.072	. . .	. . .

Table 10 Grossmann *H*-values for typical quenching conditions

Quenching medium	Grossmann value (*H*)
Poor (slow) oil quench, no agitation	0.20
Good oil quench, moderate agitation	0.35
Very good oil quench, good agitation	0.50
Strong oil quench, violent agitation	0.70
Poor water quench, no agitation	1.00
Very good water quench, strong agitation	1.50
Brine quench, no agitation	2.00
Brine quench, violent agitation	5.00
Ideal quench	(a)

(a) It is possible, with high-pressure impingement, to achieve *H*-values greater than 5.00.

found. One is a geometric notch, which includes cutting tool marks, sharp corner angles, and areas with rapid section thickness changes. The other type of stress raiser commonly found is a notch in the material, which may include intergranular effects, carbide segregation, and aggregates of impurities (Ref 36).

Although it would be desirable to eliminate all stress raisers to facilitate quench processing without any potential for cracking, this is not possible, in most cases. Instead, methods of quenching to minimize potential cracking often must be developed. Polyakov provided immersion recommendations for parts with complex shapes, where cracking potential is minimum and maximum, and these are summarized in Fig. 62 (Ref 39). The Polyakov rules for quenching such parts include (Ref 39):

- Conditions for quench cracking are most favorable if parts are immersed into the quenchant, so the perimeter of the stress raiser (P_{SC}) simultaneously touches the liquid along the entire length.
- In the case where the perimeter of the stress raiser slowly touches the quenchant at the moment of immersion in individual regions, quench cracking is reduced substantially.

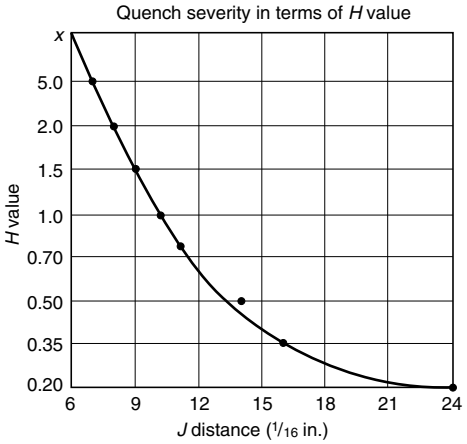

Fig. 53 Quench severity in terms of Grossman (*H*) values. *J*, Jominy distance. Source: Ref 23

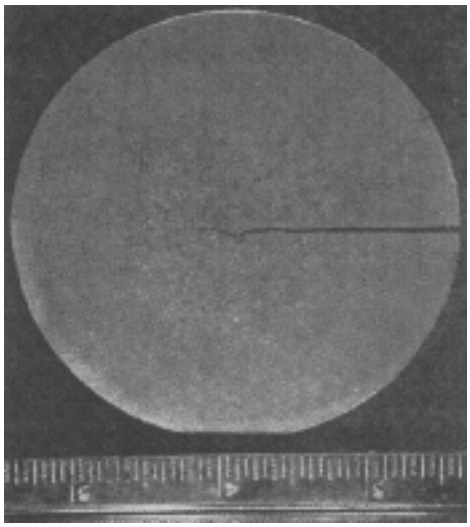

Fig. 54 Micrograph of AISI 4340 quenched and tempered steel illustrating a macroetched pure quench crack. Source: Ref 27

Retained Austenite

The austenitic structure that remains in steel after quenching is called retained austenite. The amount of retained austenite is dependent on the M_s and M_f temperatures. To obtain complete transformation, steel must be quenched into the martensitic transformation region for sufficient time for austenite to transform to martensite. If the M_f temperature is below ambient temperature, the transformation to martensite is incomplete, and some austenite is retained in the as-quenched structure. In these cases, to obtain complete transformation, the steel must be quenched directly into a refrigerant to a temperature below the M_f. However, if steel is first quenched to ambient temperature and then cryogenically cooled, additional austenite is transformed to martensite, but there is still a small fraction of retained austenite (Ref 30).

Increasing carbon content of steel increases the potential for retained austenite on quenching, as illustrated in Fig. 63 (Ref 30). This is because the M_s temperature decreases with increasing carbon content. The effect of carbon content on the M_s temperature can be calculated using the Steven and Haynes equation for steels containing up to 0.5% C (Ref 40):

$$M_s(°C) = 561 - 474C - 33Mn - 17Ni - 17Cr - 21Mo$$

where carbon, manganese, nickel, chromium, and molybdenum are concentrations of these elements in percent. For carbon concentrations greater than 0.5%, corrections must be made using Fig. 64 (Ref 30).

The M_f temperature is typically approximately 215 °C (385 °F) below the M_s (Ref 40). Typi-

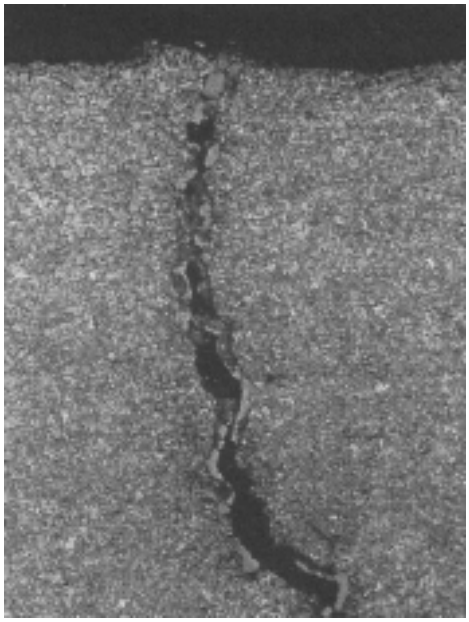

Fig. 55 Micrograph of AISI 1045 steel as quenched and tempered. Microstructure shows bands with banded tempered martensite and some bainite. The crack profile revealed evidence of tempering oxide and secondary cracking. 200×; 2% nital etch. Source: Ref 27

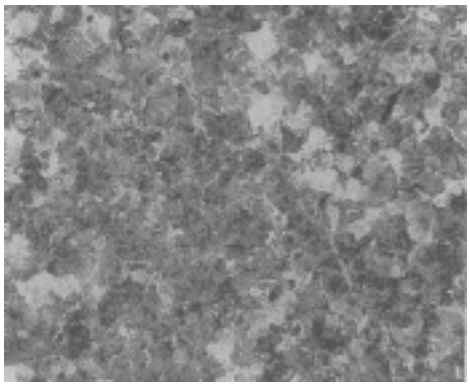

Fig. 56 Micrograph of AISI 1045 steel as quenched and tempered; representative of underheated microstructure adjacent to cracking. 376×; 2% nital etch. Source: Ref 27

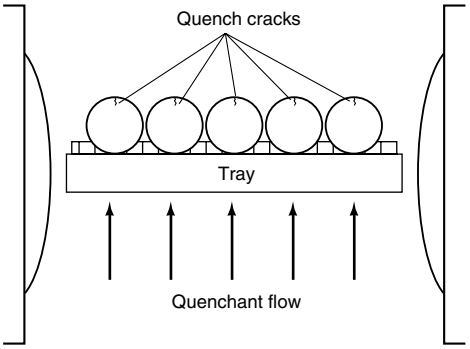

Fig. 57 Harmful effects of impeded vertical quenchant flow through the load of a batch quench system

Table 11 Comparison of typical heat transfer rates for various quenching media

Quench medium	Heat transfer rate ($W \cdot m^{-2} K^{-1}$)
Still air	50–80
Nitrogen (1 bar)	100–150
Salt bath or fluidized bed	350–500
Nitrogen (10 bar)	400–500
Helium (10 bar)	550–600
Helium (20 bar)	900–1000
Still oil	1000–1500
Hydrogen (20 bar)	1250–1350
Circulated oil	1800–2200
Hydrogen (40 bar)	2100–2300
Circulated water	3000–3500

cally, when the M_f temperature is less than the quenchant temperature, the transformation to martensite is incomplete. The volume of untransformed austenite (V_γ) is related to the M_s and the quenchant temperature (T_q) by the Koistinen and Marburger equation (Ref 41):

$$V_\gamma = \exp\left[-1.10 \times 10^{-2}(M_s - T_q)\right]$$

These equations are used to estimate the impact of steel chemistry and quenching conditions on the amount of retained austenite that may be expected.

Dimensional changes may occur slowly or fast and are due to the volume composition of the transformation products formed on quenching. One of the most important, with respect to residual stress variation, distortion, and cracking, is the formation and transformation of retained austenite. For example, the data in Table 12 indicate the slow conversion of retained austenite to martensite, which was still occurring days after the original quenching process for the two steels shown (Ref 18, 19). This is particularly a problem when dimensional control and stability is one of the primary goals of heat treatment. Therefore, microstructural determination is an essential component of any distortion-control process.

Figure 65 illustrates the microstructure of a nickel-chromium steel containing different amounts of retained austenite (Ref 30). The retained austenite resides in the interlath boundaries of martensite. The volume of retained austenite is dependent on the prior austenite grain size and the amount of austenite retained, which is dependent on the carbon content, alloying element concentration, and the quenching temperature.

The effect of retained austenite on the properties of steel can be summarized generally as (Ref 30):

- Retained austenite reduces hardness, which is proportional to the amount of retained austenite present.
- Tensile strength and yield strength decrease with increasing amounts of retained austenite.
- Because retained austenite relates to untransformed martensite, there is a reduction of maximum attainable surface compressive stresses that would have been attained if transformation to martensite was complete.
- Strength and compressive stresses are reduced by the presence of retained austenite, thus reducing fatigue resistance.
- Wear resistance decreases with increasing retained austenite.

The amount of retained austenite may be reduced by refrigeration to facilitate the transformation to martensite. Alternatively, surface-working methods, such as shot peening or surface rolling, may be used to effectively work

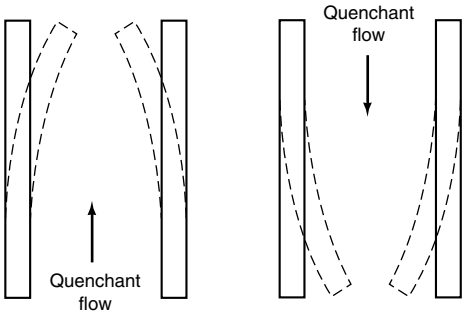

Fig. 58 Effect of quenchant flow direction on distortion

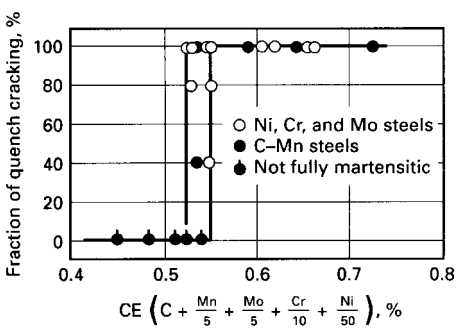

Fig. 59 Effect of M_s temperature and carbon equivalent (CE) on quench cracking of selected steels

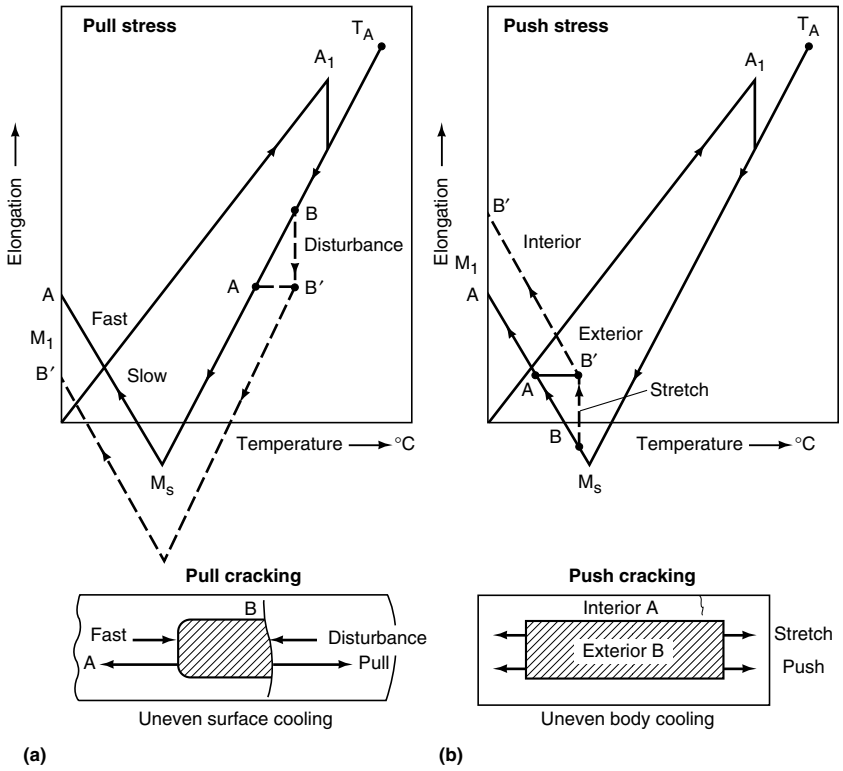

Fig. 60 Schematics of the mechanisms that generate (a) pull stress and pull cracking and (b) push stress and push cracking

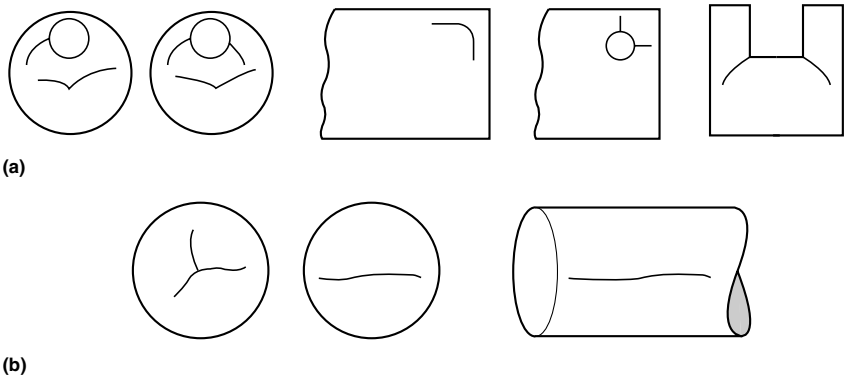

Fig. 61 Two forms of quench cracking. (a) Pull cracking (b) Push cracking

harden the surface, resulting in higher compressive stresses.

Quenching Methods

Part design, materials selection, quenchant selection, and so on are important factors for suppressing quench distortion and cracking of steel parts. In addition, several methods for minimizing distortion and eliminating cracking may also be used, for example, interrupted quenching and press quenching.

Interrupted Quenching Techniques. Interrupted quenching refers to the rapid cooling of the steel parts from the austenitizing temperature to a temperature where it is held for a specified period of time, followed by slow cooling. There are several different types of interrupted quenching: austempering, marquenching (martempering), time quenching, and so on. The temperature at which the quenching is interrupted, the length of time the steel is held at temperature, and the rate of cooling can vary, depending on the type of steel and workpiece thickness.

Marquenching (martempering) is a term used to describe an interrupted quenching from the austenitizing temperature of steels. The purpose is to delay the cooling just above the martensitic transformation temperature until temperature equalization is achieved throughout the steel part. This minimizes the distortion, cracking, and residual stress. The term *martempering* is somewhat misleading, and the process is better described as marquenching. Figures 66(a) and (b) (Ref 42) show the significant difference between conventional quenching and marquenching. The marquenching of steel consists of:

- Quenching from the austenitizing temperature into a hot quenching medium (hot oil, molten salt, molten metal, or a fluidized particle bed) at a temperature usually above the martensite range (M_s point)
- Submerging in the quenching medium until the temperature throughout the steel workpiece is substantially uniform
- Cooling (usually in air) at a moderate rate to prevent large differences in temperature between the outside and the core of the workpiece

The formation of martensite occurs fairly uniformly throughout the workpiece during the cooling to room temperature, thereby avoiding excessive amounts of residual stress. Straightening or forming is also easily accomplished on removal from the marquenching bath while the part is still hot. The marquenching can be accomplished in a variety of baths, including hot oil, molten salt, molten metal, or a fluidized particle bed. Cooling from the marquenching bath to room temperature is usually conducted in still air. Deeper hardening steels are susceptible to cracking while martensite forms, if the cooling rate is too rapid. Marquenched parts are tempered in the same manner as conventional quenched parts. The time lapse before tempering is not as critical, because the stress is greatly reduced.

The advantage of marquenching lies in the reduced thermal gradient between surface and core as the part is quenched to the isothermal temperature and then is air cooled to room temperature. Residual stresses developed during marquenching are lower than those developed during conventional quenching, because the greatest thermal variations occur while the steel is in the relatively plastic austenitic condition, and because the final transformation and thermal changes occur throughout the part at approximately the same time. Marquenching also reduces susceptibility to cracking.

Modified marquenching differs from standard marquenching only in that the temperature of the quenching bath is below the M_s point (Fig. 66c) (Ref 42). The lower temperature increases the severity of quenching. This is important for steels of lower hardenability that require faster cooling in order to harden to sufficient depth. Therefore, modified marquenching is applicable to a greater range of steel compositions than is the standard marquenching.

Austempering consists of rapidly cooling the steel part from the austenitizing temperature to a temperature above that of martensite formation, holding at a constant temperature to allow isothermal transformation, followed by air cooling. The steel parts must be cooled fast enough so that no transformation of austenite occurs during cooling and then held at bath temperature long enough to ensure complete transformation of austenite to bainite. Molten salt baths are usually the most practical for austempering applications. Parts can usually be produced with less dimensional change by austempering than by conventional quenching and tempering. In addition, austempering can decrease the likelihood of cracking and can improve ductility, notch toughness, and wear resistance. However, austempering is applicable to a limited steel and parts size. Important considerations for the selection of steel parts for austempering are:

- The location for the nose of the time-temperature-transformation (TTT) curve and the speed of the quenching

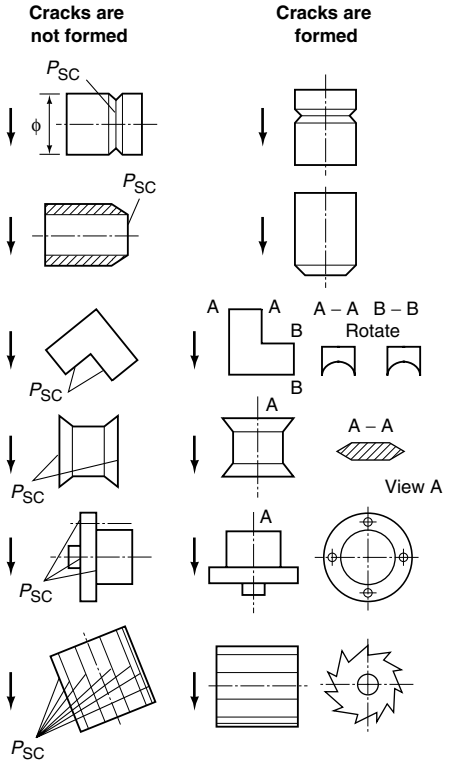

Fig. 62 Polyakov rules for immersion of cylindrical parts into a quenchant. The dashed horizontal lines indicate the level of the liquid; the vertical arrows indicate the direction of immersion of the part. P_{SC} indicates the perimeter of the stress concentrator.

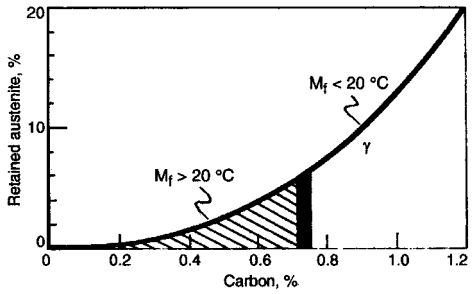

Fig. 63 Influence of carbon content on the formation of retained austenite. Source: Ref 30

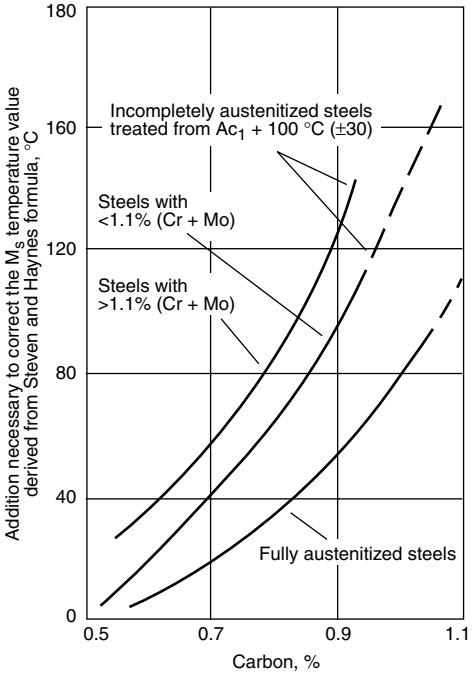

Fig. 64 Correction curves for use with the Steven and Haynes equation, with Parrish modifications indicated by dashed lines (see Ref 30). When the carbon content is less than 0.9%, an 830 °C (1530 °F) soak for greater than 2 h should produce a fully austenitic structure. Source: Ref 30

- The time required for complete transformation of austenite to bainite at the austempering temperature
- The location of the M_s point
- Maximum thickness of section that can be austempered to a fully bainite structure

Carbon steels of lower carbon content are restricted to a lesser thickness. For 1080 steel, the maximum section thickness is approximately 5 mm (0.2 in.). Low-alloy steels are usually restricted to approximately 10 mm (⅜ in.) or thinner sections, while more hardenable steels can be austempered in sections up to 25 mm (1 in.) thick. Nevertheless, sections of carbon steel thicker than 5 mm (0.2 in.) are regularly austempered in production, when some pearlite is permissible in the microstructure (Ref 43).

Time quenching is one of the interrupted quenching methods and is used when the cooling rate of the part being quenched needs to be abruptly changed during the cooling cycle. The usual practice is to lower the temperature of the part by quenching in a medium with high heat-removal characteristics (for example, water) until the part has cooled below the nose of the TTT curve and then to transfer the part to a second medium (for example, oil, air, an inert gas), so that it cools more slowly through the martensite formation range. Time quenching is most often used to minimize distortion, cracking, and dimensional changes.

Restraint Quenching Techniques. Restraint quenching refers to quenching under restraint of distortion of steel, for example, quenching by using restraint fixtures, press quenching, cold die quenching, plague quenching, and so on. There are many round, flat, or cylindrical parts that distort to an unacceptable degree by conventional immersion quenching. Under such conditions, it is necessary to resort to special techniques. However, the equipment for those special techniques is expensive, and production rates are slow. Consequently, the resulting cost of heat treatment is relatively high. Therefore, use of these techniques should be considered only when minimal distortion is mandatory. Press quenching is closely related to intense quenching, which is discussed elsewhere in this article.

Restraint fixturing is costly and is used primarily for highly specialized applications. Representative examples are the quenching of rocket and missile casings or other large components with thin wall sections.

Press Quenching and Plug Quenching. Probably the most widely used special technique is press quenching. To minimize distortion caused by the quenching cycle, press and plug quenching dies must be made to provide the proper quenchant flow and hold critical dimensions of the part being quenched. In quenching, the die or plague contacts the heated part, and the pressure of the press restrains the part mechanically. This occurs before quenching begins, while the part is hot and plastic. The machine and dies then force the quenching medium into contact with the part in a controlled manner.

Cold Die Quenching. Thin disks, long thin rods, and other delicate parts that distort excessively by conventional immersion quenching can often be quenched between cold dies with no distortion. Cold die quenching is limited to parts with a large surface area and small mass, such as washers, rods of small diameter, thin blades, and so on. Large, thin thrust washers have to be flat after quench hardening, but considerable distortions are developed as a result of blanking and machining stresses. To ensure the required flatness, the washers are squeezed between a pair of water-cooled dies immediately after leaving the furnace.

Other quenching methods include selective quenching, spray quenching, and intensive quenching.

Selective quenching is used when it is desirable for certain areas of a part to be relatively unaffected by the quenching medium. This can be accomplished by insulating an area to be more slowly cooled, so the quenchant contacts only those areas of the part that are to be rapidly cooled. A clay-coating method may be employed for selective quenching, as in, for example, the water quenching of Japanese swords. The distortion and microstructure of Japanese swords is controlled by the thickness distribution of the clay layer. A thick clay layer (>0.1 mm, or 0.004 in.) suppresses the cooling rate by its insulating effect, and a thin clay layer increases the cooling rate during water quenching by its cooling accelerating effect (Fig. 67). Selective quenching is often effective for suppressing excessive distortion or cracking.

Spray quenching involves directing high-pressure streams of liquid onto the surfaces of steel parts. Spray quenching is often useful for minimizing distortion and cracking, because it can realize a uniform quenching by selecting optimal spray condition and the sprayed surfaces where higher cooling rates are desired. The cooling rate can be faster, because the quenchant droplets formed by the high-intensity spray impact the part surface and remove heat very effectively.

Fog quenching uses a fine fog or mist of liquid droplets in a gas carrier as the cooling agent. Although similar to spray quenching, fog quenching produces lower cooling rates because of the relatively low liquid content of the stream.

Intensive quenching (Ref 44) involves forced-convection heat exchange both during high-temperature cooling and also during the transformation of austenite into martensite. Intensive quenching promotes temperature uniformity during cooling through the cross section of the part. Cooling intensity should be sufficient to promote maximum surface compressive stresses. This occurs when the Biot number ≥18. The second criterion of intensive quenching is that the

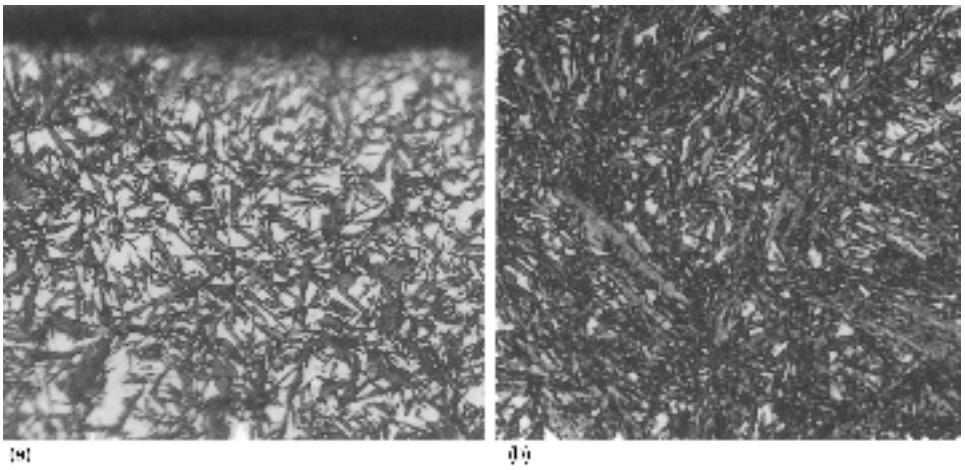

Fig. 65 Retained austenite (white) and martensite in the surfaces of carburized and hardened nickel-chromium steel testpieces. (a) Approximately 40% retained austenite. (b) Approximately 15% retained austenite. Both 550×. Source: Ref 30

Table 12 Dimensional variation in hardened high-carbon steel with time at ambient temperature

Steel type	Tempering temperature °C	Tempering temperature °F	Hardness, HRC	Change in length, % × 10^3 After 7 days	After 30 days	After 90 days	After 365 days
1.1% C tool steel (790 °C, or 1450 °F, quench)	None		66	−9.0	−18.0	−27.0	−40.0
	120	250	65	−0.2	−0.6	−1.1	−1.9
	205	400	63	0.0	−0.2	−0.3	−0.7
	260	500	61.5	0.0	−0.2	−0.3	−0.3
1% C/Cr (840 °C, or 1540 °F, quench)	None		64	−1.0	−4.2	−8.2	−11.0
	120	250	65	0.3	0.5	0.7	0.6
	205	400	62	0.0	−0.1	−0.1	−0.1
	260	500	60	0.0	−0.1	−0.1	−0.1

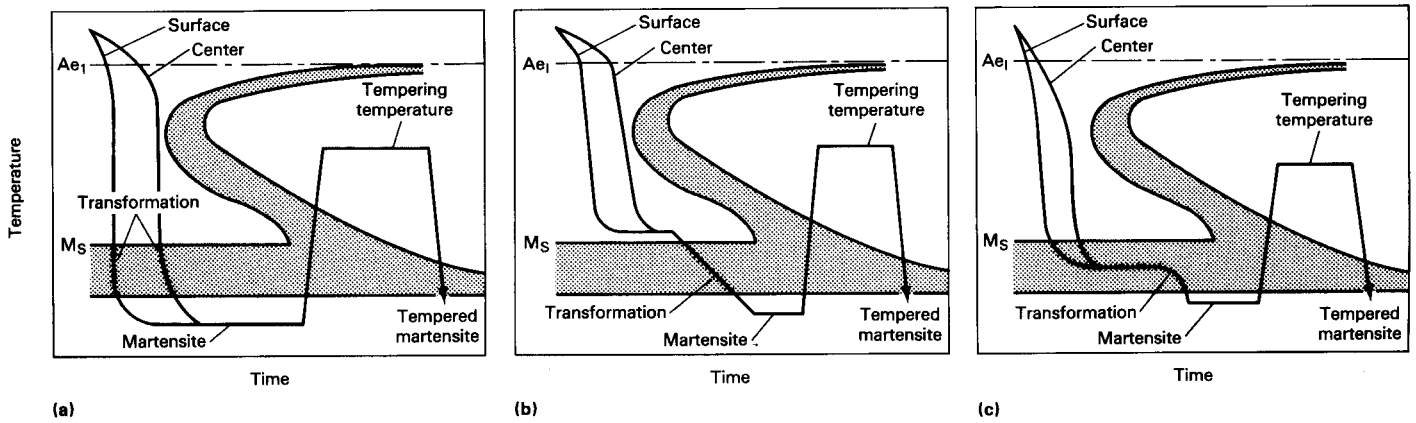

Fig. 66 Comparison of cooling curves as a workpiece cools into and through the martensite transformation range for a conventional quenching and tempering process and for interrupted quenching processes. (a) Conventional quenching and tempering. (b) Marquenching. (c) Modified marquenching. Ae_1, austenite start transformation under equilibrium conditions

intensive cooling be stopped at the moment that maximum surface compressive stresses are formed.

Steel Transformation Products and Properties

Internal oxidation, also called subscale formation, is the formation of corrosion product particles below the surface of the metal. Internal oxidation has a deleterious effect on hardness, bending fatigue strength, residual stresses, and wear resistance.

Internal oxidation occurs preferentially with certain alloy constituents, primarily manganese, chromium, and silicon, by inward diffusion of oxygen, sulfur, and other gases to the site of oxidation during carburizing using an endothermic atmosphere at 900 to 950 °C (1650 to 1740 °F). An endothermic atmosphere (endogas) is produced by the controlled combustion of a hydrocarbon gas, such as natural gas and propane, with air. The oxygen required for internal oxidation is derived primarily from carbon dioxide and water vapor, the by-products of the combustion process. Figure 68 shows the oxidation potential of various alloying elements in an endothermic gas (Ref 30).

It is essentially impossible to eliminate internal oxidation when carburizing using an endothermic atmosphere. The presence of approximately 0.25% Si in carburizing grades of steel far exceeds the amount necessary to produce internal oxidation. In addition, the presence of silicon also reduces the threshold concentrations of manganese and chromium that produce internal oxidation. However, the sensitivity to internal oxidation may be decreased by the presence of alloying elements with atomic numbers greater than iron, such as nickel and molybdenum.

The oxygen content and depth of oxygen penetration increase with increasing oxygen potential (concentration) at a particular temperature. However, the depth of penetration increases with both temperature and time, as shown in Fig. 69 (Ref 30). Because the oxygen potential decreases with increasing carbon potential, the amount of internal oxidation is less at higher-carbon-potential carburizing processes, depending on the carburizing time.

Metallographically, there are two common forms of internal oxidation observed. The first type appears as globular particles of approximately 0.5 μm in diameter from nearest to the surface to a depth of approximately 8 μm. Although these oxides may occur along the surface, they usually are found in the grain and subgrain boundaries and possibly within the grain. If the oxidation occurs on the surface, the grains are typically 0.5 to 1 μm, although they may be as large as 2 to 4 μm (Ref 38).

The second type of internal oxides occurs at greater depths, typically 5 to 25 μm and appear

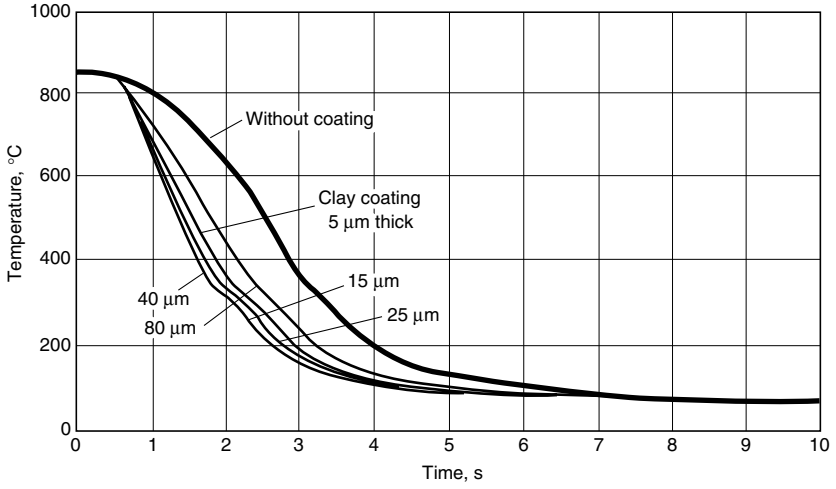

Fig. 67 Effect of clay coating on cooling curves of steel test specimen quenched into still water at 30 °C (86 °F). Test specimen, JIS S45C steel cylinder (10 mm, or 0.40 in., diam × 30 mm, or 1.2 in., long)

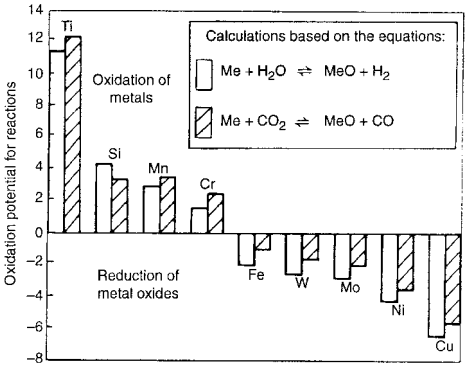

Fig. 68 Oxidation potential of alloying elements and iron in steel heated in endothermic gas with an average composition of 40% H_2, 20% CO, 1.5% CH_4, 0.5% CO_2, 0.28% H_2O (dewpoint, 10 °C, or 50 °F), and 37.72% N_2. Source: Ref 30

as a dark phase at prior austenite grain boundaries, as illustrated in Fig. 70 (Ref 30, 45). Thus, surface grain size also influences the amount of internal oxidation. As the grain size increases, the potential for internal oxidation within the grains increases (Ref 30).

Internal oxidation is also affected by the surface condition of the material being carburized, because organic impurities, such as lubricants, can contaminate the furnace atmosphere, and the presence of oxides due to scale or corrosion affect the formation and depth of penetration of internal oxidation. Although surface oxides may be removed by electropolishing, electrochemical machining, honing, grinding, shot blasting, or peening, these methods must be selected with care, because they may induce such negative effects as increased tensile stresses, risk of inducing decarburization during subsequent reheating processes, or these processes may not allow precise control.

Table 13 provides the maximum acceptable depth of internal oxidation relative to the case depth for carburized gears. (See also International Organization for Standardization (ISO) 6336-5.2; the equivalent grades are ML, MQ, and ME.) Note that grade 1 has no specification value. Also, recovery by shot peening is acceptable, with agreement of the customer.

Alloy Depletion. Another source of nonhomogeneous steel composition is alloy depletion. As with nonmetallic inclusions, alloy depletion leads to greater stresses and cracking, as illustrated in Fig. 71 (Ref 27). Examples of alloys particularly susceptible to alloy depletion are AISI 4100, 4300, and 8600 series.

High-temperature transformation products (**HTTP**) are products that form on the surface of a carburized part within the same area where internal oxidation occurs. High-temperature transformation products are nonmartensitic microstructures that include pearlite, upper and lower bainite, or mixtures of two or more of these products. A lean-alloy steel or large cross section favors pearlite at the surface, whereas higher-alloy steel or thinner cross section favors the formation of bainitic microstructures when quenched. However, if the cooling rate is sufficiently fast or if sufficient quantities of reducing elements, such as nickel and molybdenum, are within the oxide-forming region, it is possible that no HTTP is formed (Ref 30, 46).

The formation of internal oxidation products effectively results in localized depletion of the elements that are preferentially oxidized, such as manganese and chromium. When HTTP are present, they often extend deeper than the internal oxidation, especially with leaner steel grades. The occurrence of HTTP results in lower hardness, reduction of surface compressive stresses, reduction of bending fatigue, and reduction of wear resistance.

The effects of HTTP can be controlled by (Ref 30):

- Using a steel grade with sufficient alloy content in the depleted layer to give martensite on quenching
- Reducing the amount of HTTP in the surface layer by a late increase of carbon potential or a late addition of ammonia to the furnace chamber
- Using a faster quench to suppress HTTP formation; however, beware of possible increased distortion
- Removing HTTP by grinding, grit blasting, and/or shot peening

Decarburization is defined as "a loss of carbon atoms from the surface of a workpiece, thereby producing a surface with a lower carbon gradient than at some short distance below the surface" (Ref 30). This is important, because the strength of steel is dependent on carbon content (carbides) within the steel structure. If surface carbon is greater than 0.6%, the surface hardness should be acceptable. If surface carbon is approximately 0.6% or less, all the main properties are adversely affected; for example, bending fatigue could be reduced by 50%.

The depth of decarburization is defined as "the thickness of the layer in which the structure differs significantly from that of the core." Complete decarburization results in a completely ferritic microstructure within the surface layer. The depth of decarburization is the thickness of this layer. In the zone of partial decarburization, there is a gradual increase of carbon content within the ferritic layer to the core. Decarburization is observed metallographically. Figure 72(a) illustrates complete decarburization on the surface of 1018 steel. Figure 72(b) illustrates partial decarburization (Ref 30).

Carbon may also be oxidized under the same conditions leading to metallic oxidation (scaling). Therefore, although decarburization may occur independently of scaling, they typically occur simultaneously. During carbon oxidation, gaseous by-products (CO and CO_2) are formed. Usually, the most important factor controlling the rate of decarburization is the diffusion rate of carbon within the metal that must replace the carbon lost due to volatilization.

Although decarburization may occur at temperatures above 700 °C (1290 °F), decarburization is typically most severe when steel is heated to temperatures above 910°C (1670 °F) (Ref 47).

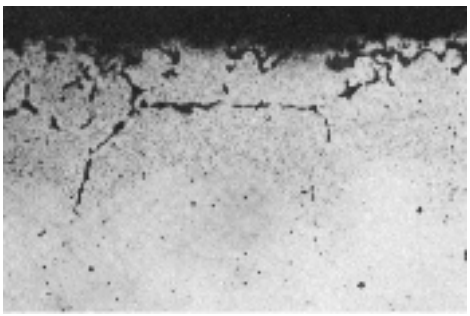

Fig. 69 Internal oxidation of a nickel-chromium steel carburized in a laboratory furnace, showing both grain-boundary oxides and oxide precipitates within grains. 402×. Source: Ref 30

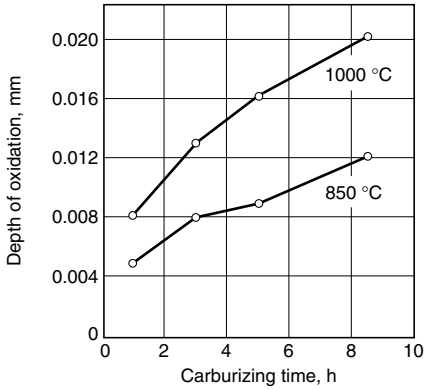

Fig. 70 Depth of oxidized zones as a function of carburizing time at different carburizing temperatures for SAE 1015. Source: Ref 30

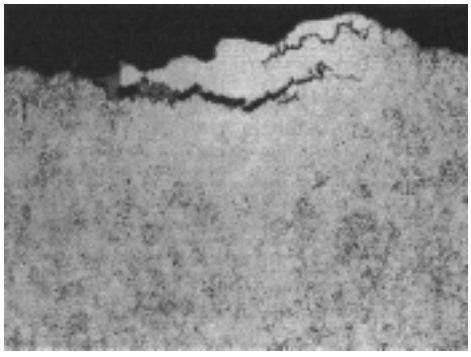

Fig. 71 Micrograph of AISI 4140 steel as quenched and tempered; microstructure is tempered martensite, where cracking is promoted by alloy depletion. 91×; 2% nital etch. Source: Ref 27

Table 13 American National Standards Institute/American Gear Manufacturers Association (ANSI/AGMA) 2001-C95 standard values for acceptable depth of internal oxidation for carburized gears relative to case depth (tooth size)

Grade 2		Grade 3		Case depth	
mm	in.	mm	in.	mm	in.
0.0178	0.0007	0.0127	0.0005	<0.75	<0.030
0.0254	0.0010	0.0203	0.0008	0.75–1.50	0.030–0.059
0.0381	0.0015	0.0203	0.0008	1.50–2.25	0.059–0.089
0.0508	0.0020	0.0254	0.0010	2.25–3.00	0.089–0.118
0.0610	0.0024	0.0305	0.0012	>3.00	>0.118

The depth of decarburization actually depends on both temperature and time, as shown in Fig. 73 (Ref 30).

Exothermic atmosphere (exogas) is used as a protective atmosphere to prevent decarburization, scaling, and other undesirable surface reactions. To achieve the best results, the dewpoint must be minimized. This is accomplished by drying the gas. The relationship between dewpoint and carbon potential (concentration) is shown in Fig. 74 (Ref 30).

The effects of decarburization may be corrected, depending on the degree of decarburization. Shot peening may be used for shallow decarburization or partial decarburization. For deeper total decarburization or partial decarburization, a process called restoration carburizing may be used, but it is usually accompanied by some additional distortion.

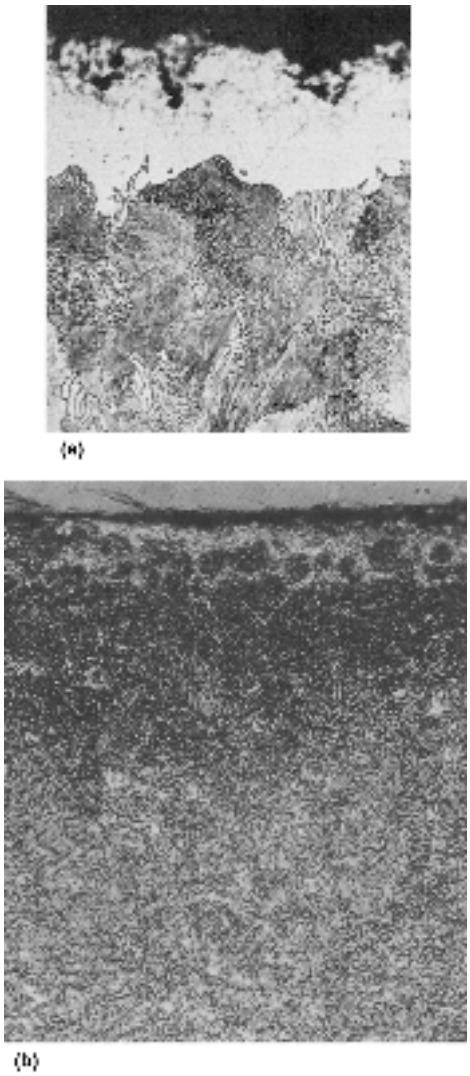

Fig. 72 Micrographs showing different degrees of decarburization. (a) Total decarburization caused by a furnace leak during gas carburizing of AISI 1018 steel. 500×; 1% nital etch. (b) Partially decarburized specimen. 190×. Source: Ref 30

A specification for decarburization is ANSI/AGMA 2001-C95. There are no specification limits for grade 1. For grades 2 and 3, no partial decarburization is apparent in the outer 0.13 mm (0.005 in.), except in unground roots. Another standard for decarburization is ISO 6336-5.2. For MQ and ME grades, the reduction of surface hardness due to decarburization in the outer 0.1 mm (0.004 in.) should not exceed 2 HRC on the test bar.

Carbides. When the carbon content is greater than the eutectoid carbon content, free carbides may form when the steel is heated above the austenite formation temperature (Ac_1) or when they are rejected by austenite during cooling and before the austenite-pearlite, austenite-bainite, or austenite-martensite transformations occur. Depending on the steel composition and processing conditions, free carbides may appear metallographically as networks, spheroids or large chunky particles, or as surface films (Ref 30). Different geometric models for carbide formation are shown schematically in Fig. 75 (Ref 48).

So-called "massive carbides," as illustrated in Fig. 76, may be formed under isothermal conditions at austenite grain junctions. Under these conditions, carbides are formed in three directions by step and ledge growth mechanisms, where ledge heights are much greater than step heights, as illustrated in Fig. 75(a).

After diffusion to austenite grain boundaries below the Ac_{cm} temperature, excess carbon is deposited to form a film of small, thin platelets, which are illustrated in Fig. 77 (Ref 30). Although the ledges and steps are of heights similar to those producing massive carbides (Fig. 75(b)), they differ by the temperatures at which they are formed. These carbides may appear as isolated grain-boundary particles forming a row with a film length that is equivalent to the prior austenite grain boundary. This film carbide is a continuous carbide network and is illustrated in Fig. 78 (Ref 30). A fine grain size may reduce the amount of carbon deposited at the grain boundaries. Lean-alloy grades with high manganese contents may be more prone to developing network carbides.

Intergranular carbides, which precipitate on planes within the grains, exist in a cylindrical pattern and a smooth spiraling surface, as shown in Fig. 75(c).

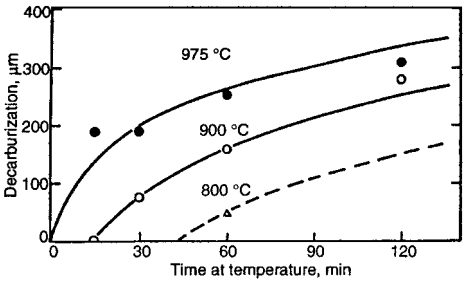

Fig. 73 Depth of decarburization of a cold-worked steel in a fluidized bed in air. Source: Ref 30

Network and dispersed carbides, while harder than martensite, typically exist in concentrations <10% to exhibit any significant effect on macrohardness. Surfaces containing network carbides exhibit tensile macroresidual stresses (Ref 49). However, spheroidal carbides exhibit compressive macroresidual stresses (Ref 49).

Continuous network carbides reduce bending fatigue strength, whereas partial carbide networks do not exhibit any significant effect (Ref 50). Even under controlled carburizing conditions, carbide buildup can occur at external edges and corners. For example, corner carbides can reduce bending fatigue strength, depending on the concentration and type of carbide formed. Interestingly, the effect can be eliminated by rounding the corners and edges before carburizing (Ref 30). Increasing network carbide concentrations improved high-stress/low-cycle rolling-contact fatigue (Ref 50).

Globular carbide dispersions, such as those illustrated in Fig. 79, are formed by slowly heating a steel surface through the Ac_1 to the ferrite-to-austenite tranformation completion (Ac_3) temperatures in the presence of a carburizing atmosphere (Ref 30). Film carbides or flake carbides, illustrated in Fig. 80 (Ref 30), exist as a continuous or discontinuous film on the surface of a carburized part. In gas carburizing, this carbide structure forms due to cooling from the carburizing temperature in an atmosphere with a high carbon potential.

Because carbides are hard, high surface-carbide concentrations should exhibit hardness values significantly higher than noncarbide-containing surfaces. The term *supercarburizing* is a carburizing process conducted at 930 °C (1710 °F) in a high carbon potential with subsequent subcritical annealing to a temperature just below the Ac_1 temperature; the process is repeated and finally quenched and tempered (Ref 51). This

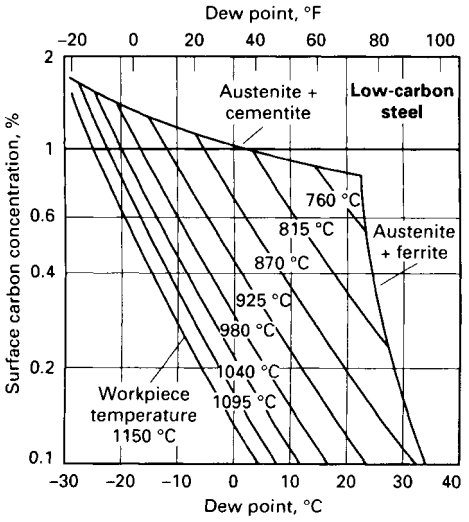

Fig. 74 Variation of carbon potential with dewpoint for an endothermic-based atmosphere containing 20% CO and 40% H_2 in contact with plain carbon steel at various steel temperatures. Source: Ref 30

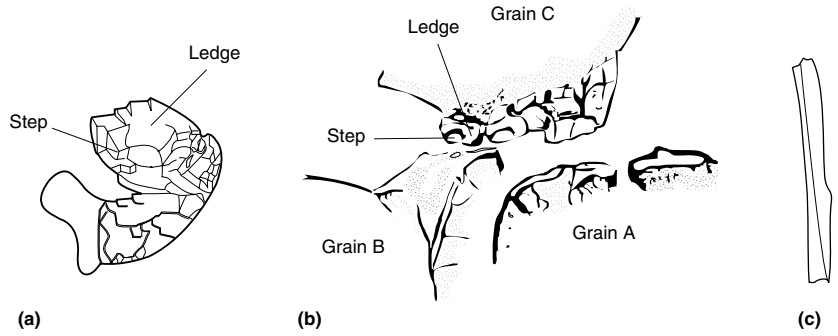

Fig. 75 Geometric models of carbides formed during case hardening. (a) Massive carbide grain, 4000×. (b) Film carbide, 2000×. (c) Intergranular carbide, 4000×. Source: Ref 30

process results in surface carbon contents of 1.8 to 3% and greater than 25% carbides. Supercarburized parts exhibit up to 15% better bending fatigue properties. Coarse carbide structure may result in significantly reduced contact fatigue (Ref 30). Wear resistance generally increases with increasing carbide concentration.

Carbide particles may be unavoidably formed during reheat-quenched carburized alloy steels. These dispersed, fine particles generally do not produce detrimental effects and may even be unavoidable in reheat-quenched carburized alloy steels. However, massive carbides, which may be formed at grain boundaries in the outer 0.05 mm (0.002 in.) at corners and edges, may be detrimental. Network carbides, which are formed during posthardening processes, can be detrimental to properties.

Influential Microstructural Features

Grain Size. The mechanical properties and toughness of steel, both in the case and core if the steel is carburized, are not only affected by carbon and alloying element concentration and microstructure but also by the grain size. Typically, finer grain sizes are preferred. The ASTM grain size characterization comparison is illustrated in Fig. 81 (Ref 30).

Figure 82 illustrates the effect of increasing temperature on grain size (Ref 47). The following are reasons for grain growth when the temperature was increased from 850 to 1250 °C (1560 to 2280 °F) (Ref 52):

- Grain resorption occurs at 50 to 100 °C (90 to 180 °F) above Ac_3
- New boundaries and grains are formed at 250 to 300°C (450 to 540 °F) above Ac_3
- Although boundary migration occurs at all temperatures, it only affects grain growth above 1100 °C (2010 °F).

If the fractured surface of a steel tool or machine component is coarse grained, this often indicates the use of excessively high austenitizing temperatures during heat treatment, or that an incorrect heat treatment for a given steel grade

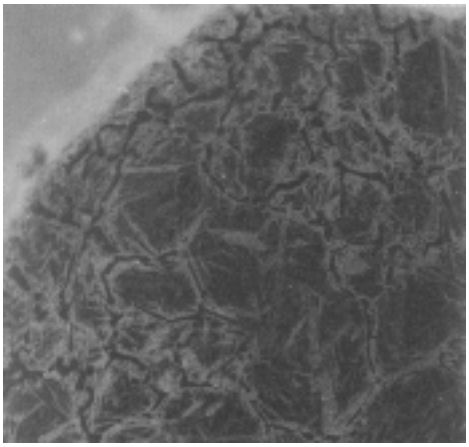

Fig. 76 Micrograph of 4% Ni-C-Cr carburized steel showing massive carbides produced during carburizing with surface carbon above Ac_{cm} carbon. Source: Ref 30

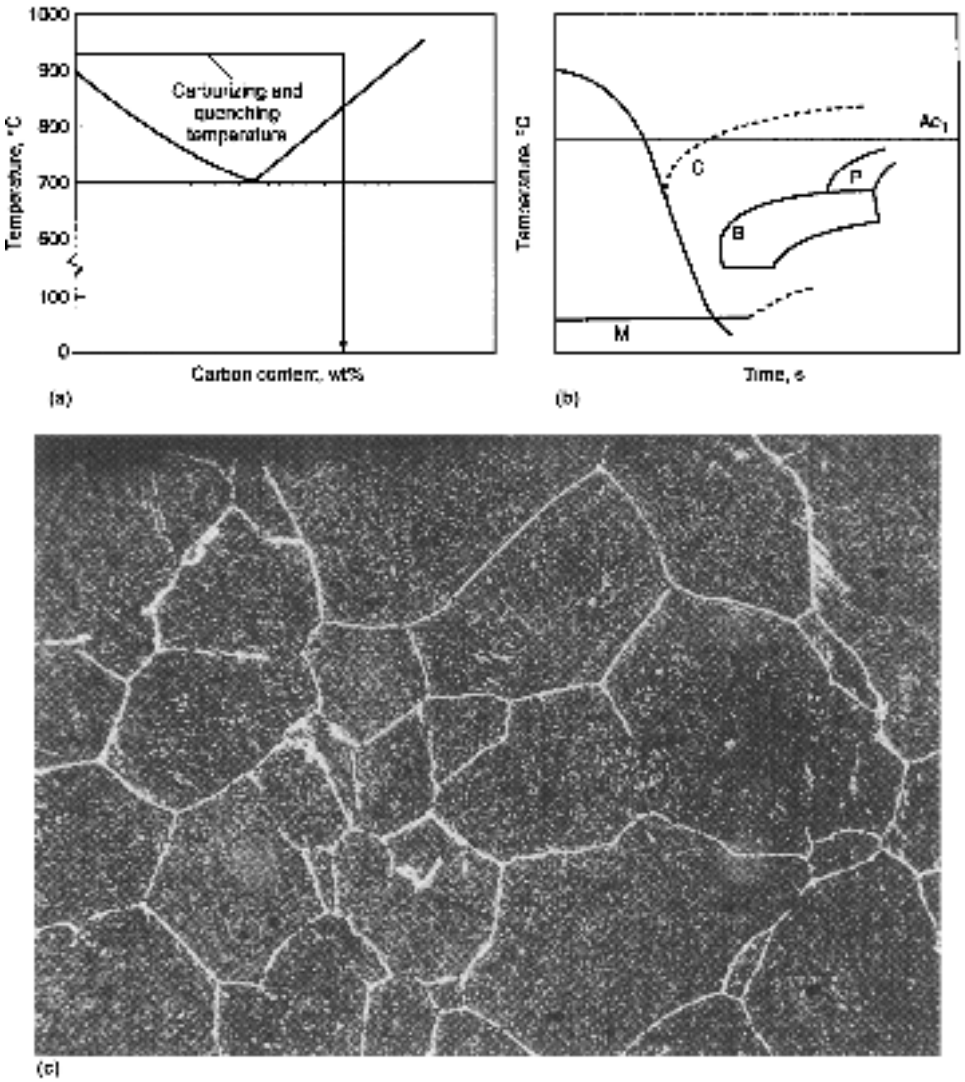

Fig. 77 Direct quenching from carburizing temperature. (a) Phase diagram schematic. (b) Continuous cooling transformation curve for a high-carbon surface. (c) Micrograph of direct quenched 3% Ni-Cr carburized steel. 280×. Source: Ref 30

was used. This is a problem, because many properties of steel are affected by grain size.

Grain growth is affected by steel composition. Steels containing alloying elements such as aluminum nitride (AlN), which inhibits grain growth, are called fine-grained steels. Fine-grained steels do not exhibit grain growth, except at relatively high austenitizing temperatures when grain growth occurs rapidly, as illustrated in Fig. 83 (Ref 30). Coarse-grained steels contain silicon, and typically, the grain size increases slowly with increasing temperature, as illustrated in Fig. 83 (Ref 30).

Grain size may be reduced (grain refinement) by normalizing, which involves heating the steel to its austenitizing temperature, holding for 10 to 20 min, and then cooling in air. Typically, normalizing produces a uniform and smaller grain size.

A fine grain size may exhibit an adverse influence on the case and the core hardenability of lean-alloy carburizing steels. However, a fine grain size is generally preferred. Coarse-grained steels may exhibit greater distortion during heat treatment (Ref 30). An as-quenched coarse austenite grain produces large martensite plates and large austenite volumes. This is important, because large martensite plates are more prone to microcracks than are small plates. These structural effects reduce fatigue and impact strengths.

Microcracks refer to cracks that develop during the formation of plate martensite. Microcracking is most often observed when the martensite plates are long and thin. Microcracking does occur in lath martensite. Microcracks are formed when the strains generated at the tip of a growing martensite plate are sufficient to produce cracking within the plate or boundary between growing plates (Ref 30). Therefore, microcracks run across the plate or alongside of the plate. They have also been observed at prior austenite grain boundaries. They are confined to the high-carbon regions of the case. Large, high-carbon martensite plates are more likely to have microcracks. Microcracks in nickel-chromium steel are shown in Fig. 84 (Ref 30).

The propensity for microcracking increases as the carbon content of the steel increases above 0.6%. Microcracking potential increases with the amount of carbon in solution in the martensite, which increases as the temperature increases from Ac_1 up to 920 °C (1690 °F). Direct quenching retains more carbon in solution in the martensite; therefore, quenching method and temperature are important. Plain-carbon and very lean-alloy grades of steel are more prone to microcracking during case hardening. However, 8620 and 52100 are known to be susceptible to microcracking (Ref 30). The frequency and size of microcracks increased with grain size (Ref 53). Microcracking has been reported to be aggravated by the presence of hydrogen (Ref 54), and tempering, even at temperatures as low as 180 °C (360 °F) for 20 min, has been reported to exhibit a healing effect (Ref 55).

Although the presence of microcracks may potentially cause various problems, there are few studies reported in this area. It is possible that fatigue strength is reduced by as much as 20% (Ref 30). Similarly, there are few standards. There are no ANSI/AGMA specifications for grades 1 and 2. For the grade 3 quality, ten microcracks in a 0.06 mm^2 (0.0001 $in.^2$) field at 400× is specified.

Microsegregation always occurs in processes such as casting. The amount of microse-

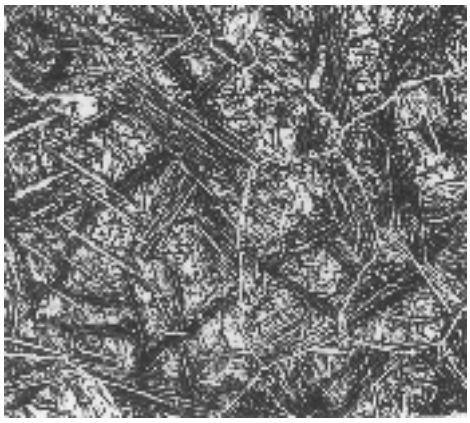

Fig. 78 Micrograph of 4% Ni steel showing carbides formed after slow cool from carburizing temperature. 178×. Source: Ref 30

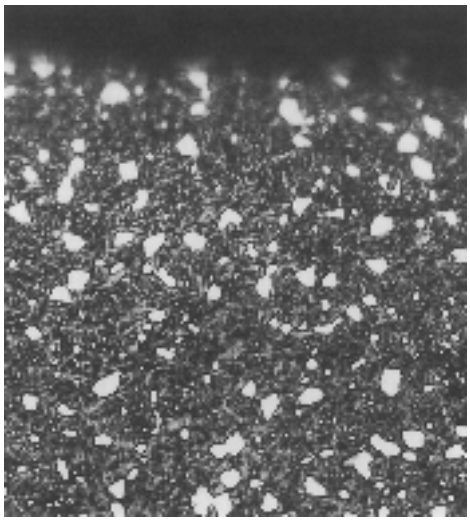

Fig. 79 Globular carbides at the surface of a carburized 1% Cr-Mo steel (reheat quenched). 836×. Source: Ref 30

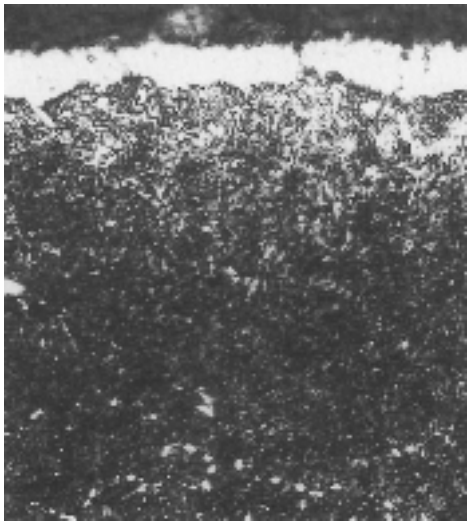

Fig. 80 Surface film carbide (1% Cr-Mo steel). 874×. Source: Ref 30

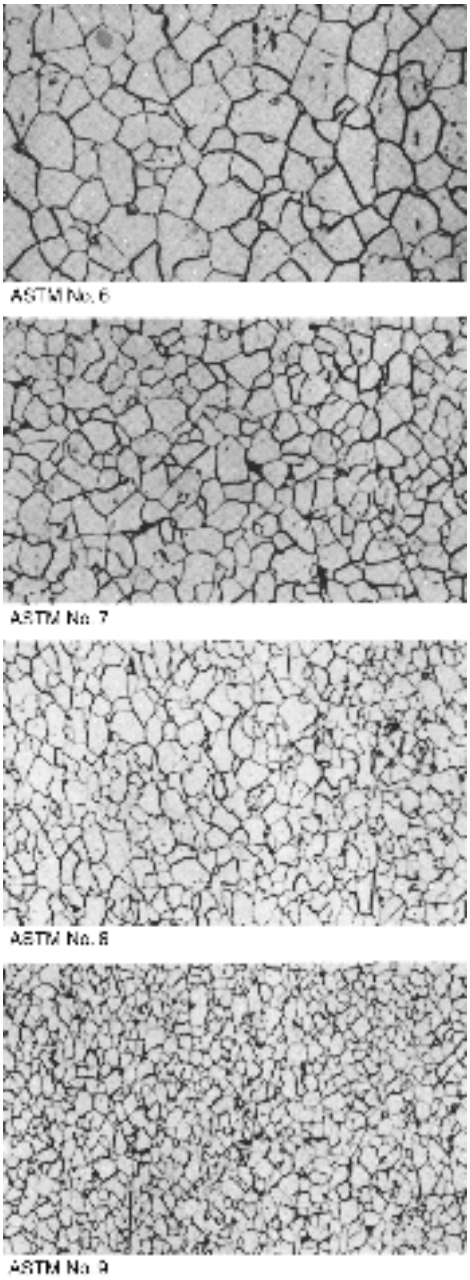

Fig. 81 Comparison of ASTM 6 to 9 grain size microstructures. 100×; nital etch. Source: Ref 30

gregation in steel castings is affected by the alloy content of the steel, including tramp elements. The propensity for microsegregation is alloy-dependent. Silicon and manganese affect the microsegregation of molybdenum, and manganese affects the microsegregation of sulfur. In addition to microstructural analysis, elemental analysis may also provide an invaluable insight into potential for inclusion formation. For example, sulfide inclusions may be obtained if insufficient manganese is present. Generally, the manganese content should be approximately five times the sulfur content to convert sulfur to manganese sulfide. The order of microsegregation susceptibility (from most to least) is sulfur, niobium, phosphorus, tin, molybdenum, chromium, silicon, manganese, and nickel (Ref 30). Figure 85 illustrates dendritic microsegregation of a fractured gear tooth (Ref 30).

Steel cracking may result from chemical segregation, which may be evident in the form of banding, as shown in Fig. 86 (Ref 27) Microstructural analysis showed that bands of tempered martensite were associated with bands of tempered martensite and bainite. The bainite appeared to originate from carbon and manganese segregation within the material, which would lead to increased internal stresses. Both surface and subsurface cracking was observed. Figure 87 shows subsurface cracking, which appeared to be intergranular (Ref 27).

In a similar case, AISI 1144, a resulfurized steel, pins with subsequent cracking at the pin tips were accompanied with soft spotting. (The pins were through-hardened prior to induction hardening of the pin tip.) Microstructural analysis showed that the cracking and soft spotting condition was due to stringer inclusions, with bands of gross chemical segregation significantly greater than normally observed with this grade of steel. The stringers act as stress concentration sites for crack initiation in the presence of quenching stresses.

Mechanical and thermal treatments may substantially affect the distribution and directionality of microsegregation, and, in some cases, it may be reduced significantly. However, because of the long soaking times required to completely homogenize the steel, it is generally recommended that nothing be done.

Microsegregation may lead to machining problems, and severe cracking in the more alloyed carburizing grades of steel may occur during slow cooling from the carburizing temperature. In carburized and quenched steels, microsegregation may lead to unsatisfactory zones of martensite and austenite. Austenite-martensite or martensite-bainite banding probably reduces fatigue resistance, especially if bainite is present. Microsegregation may also influence the growth and distortion of a part during heat treatment. Microsegregation, along with nonmetallic inclusions, influences the transverse toughness and ductility of wrought steels.

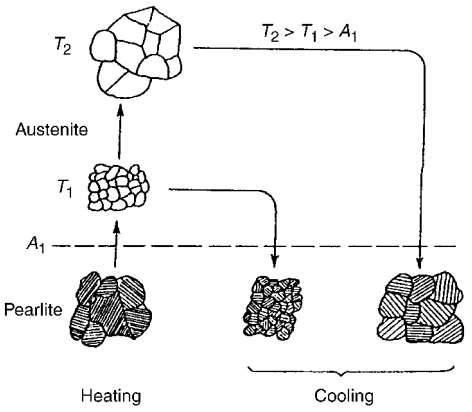

Fig. 82 Schematic illustration of the effect of austenitizing temperature on grain size of a eutectoid steel after normalizing. Source: Ref 47

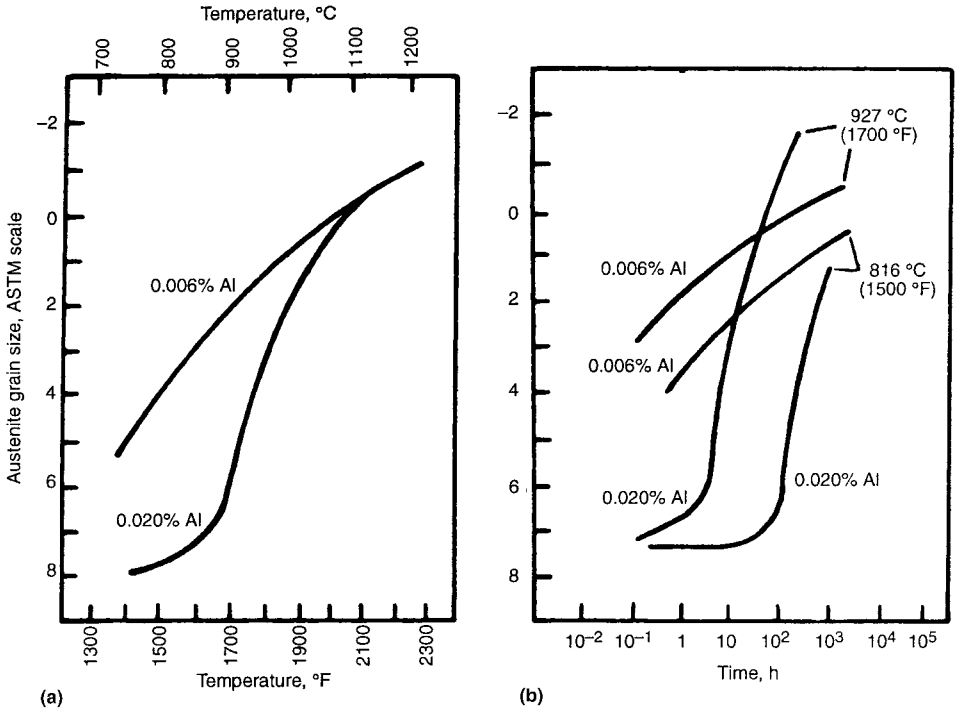

Fig. 83 Relationship between austenitization processing parameters and grain size for a grain-refined and non-grain-refined AISI 1060 steel. (a) Effect of austenitization temperature and 2 h soaking time. (b) Effect of austenitizing time. Source: Ref 30

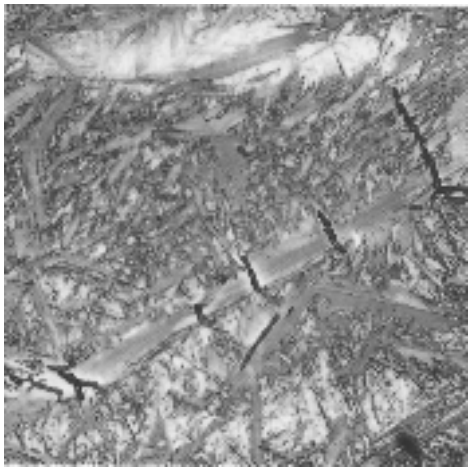

Fig. 84 Microcracking in a nickel-chromium steel that also exhibits microsegregation. 910×. Source: Ref 30

Fig. 85 Dendritic microsegregation in a fractured gear tooth. 2×. Source: Ref 30

Effects of Grinding. A properly designed case-hardening process should produce surface microstructures containing essentially fine, tempered martensite with minimal part-to-part and batch-to-batch variation. However, grinding may be performed to achieve the desired dimensions and surface finish. It is also performed to remove undesired metallurgical products resulting from heat treatment, such as carbide films and internal oxidation. However, the grinding process can unacceptably heat a surface, leading to grinding burns and even cracking. A grinding burn occurs when the part becomes sufficiently hot, as a result of the grinding action, to cause discoloration or to exhibit a microstructural change due to tempering or hardening. The temperature distribution and associated microstructure products during grinding are illustrated in Fig. 88 (Ref 30).

There are different types of grinding burns. One type results in localized tempering and is called overtemper burning. This occurs when heat is not transferred from the grinding surface sufficiently to prevent induced tempering of the martensitic surface. This results in a loss of hardness on the burned surface and possibly a loss of compressive stresses.

If the surface temperature during grinding exceeds the Ac_3, a thin layer of austenite is formed that is cooled by the mass of the part to form a light-etching martensite. This is called a rehardening burn. Because of the thermal process, the rehardened material is surrounded by overtem-

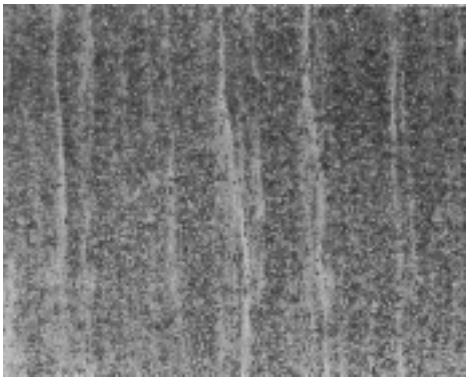

Fig. 86 Micrograph of AISI 4140 steel as quenched and tempered, showing bands of tempered martensite and tempered martensite/bainite. 50×; 2% nital etch. Source: Ref 27

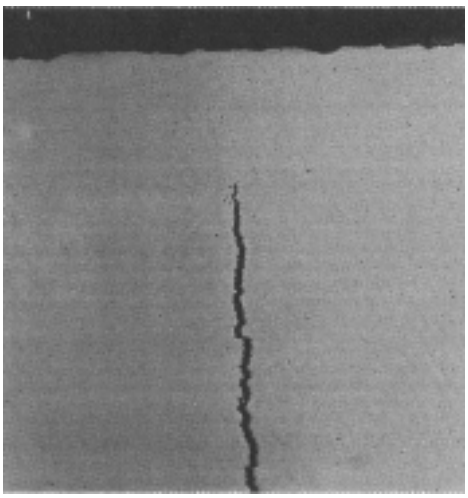

Fig. 87 Micrograph of AISI 4140 steel as quenched and tempered. Microstructure shows banded martensite and tempered martensite/bainite. Subsurface cracking is illustrated. 100×; 2% nital etch. Source: Ref 27

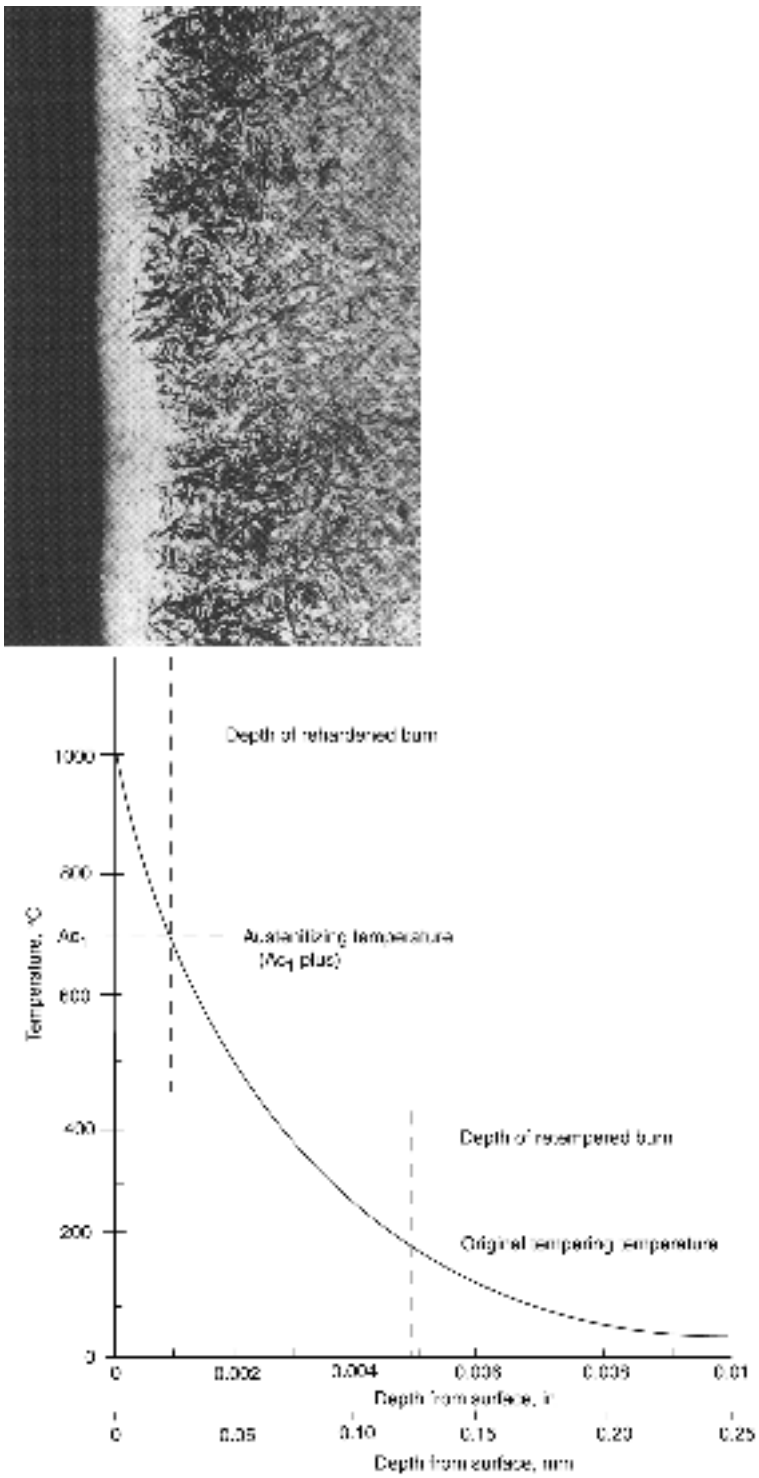

Fig. 88 Temperature distribution within a ground surface, as indicated by microstructural modifications. The Ac temperature indicated is for slow heating; at high heating rates, such as encountered in grinding, the Ac temperatures are elevated. 500×. Source: Ref 30

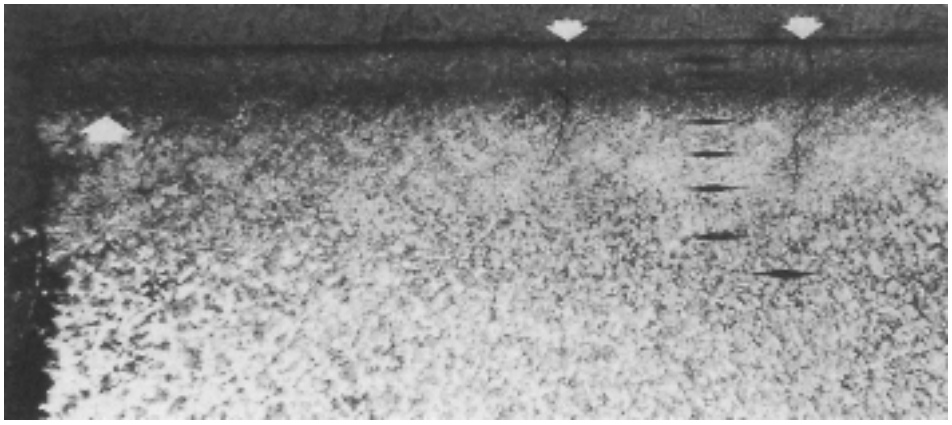

Fig. 89 Micrograph of grinding cracks in case-hardened 8620 steel showing small cracks (see small arrows) that passed through the hardened case to the core, and the burned layer on the surface (dark band with arrow at the left) that resulted in grinding burns. (Note: Nital and acidic ferric chloride are suitable etchants for grinding burns.) Source: Ref 30

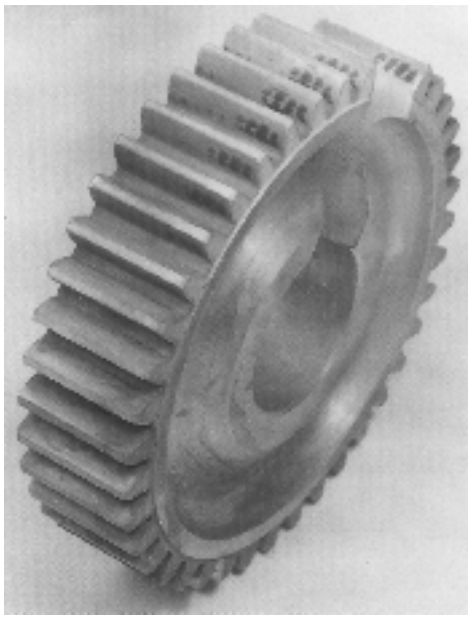

Fig. 90 Grinding cracks on the flanks of a small spur gear wheel. Source: Ref 30

pered steel and reduced hardness, as illustrated in Fig. 88 (Ref 30).

Grinding cracks, such as those illustrated in Fig. 89 and 90 are often accompanied by grinding burns (Ref 30). Grinding cracks typically form perpendicular to the grinding direction and penetrate at right angles to the surface. It is possible for the crack to penetrate substantially deeper than the depth of the burn.

When grinding, the grinding wheel grade, wheel speed, and depth of cut are important process considerations. Generally, it is recommended to locate the high spots and then proceed with light cuts. If wet grinding is done, ensure that coolant feed is adequate and correctly directed. The part should be inspected for grinding burns, cracks, and steps in gear tooth fillets. Ground surfaces vary from good quality (with compressive residual stresses) to poor quality (with burns or even cracks). Bending fatigue strength is improved or seriously impaired, depending on the quality of the ground surface. Because grinding improves the contact accuracy and surface smoothness, the quality of this process affects lubrication and contact fatigue. Tempering and peening may be used to improve the quality of ground surfaces.

The following example illustrates the potential impact of grinding cracks. An AISI G-3500 gray iron camshaft was induction hardened to a depth of 1.5 to 3.8 mm (0.060 to 0.150 in.) and a lobe hardness of 45 HRC. Cracking was observed by magnetic-particle inspection of the cam lobe after subsequent machining. Elemental analysis showed that the carbon content of the steel was higher than the specification value (3.56% C versus 3.10 to 3.45% C). The surface hardness was 52 HRC versus a specification value of 45 HRC. The hardness was 94 HRB. Microstructural evidence suggested quenching from an excessively high austenitizing temperature, which contributed to the formation of excessive amounts of retained austenite at the core lobe surface and within the induction-hardened case. Grinding stresses, apparently caused during machining of the cam lobe surface, apparently caused localized martensitic transformation of the retained austenite. Cracking that occurred due to the martensitic conversion is shown in Fig. 91 (Ref 27).

Effects of Shot Peening. Shot peening improves surface hardness and induces compressive stresses. This is essentially a cold working

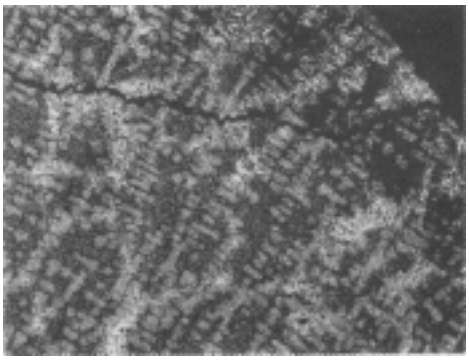

Fig. 91 Micrograph of induction-hardened AISI G-3500 gray iron illustrating crack propagation into the hardened case. 88×; 3% nital etch. Source: Ref 27

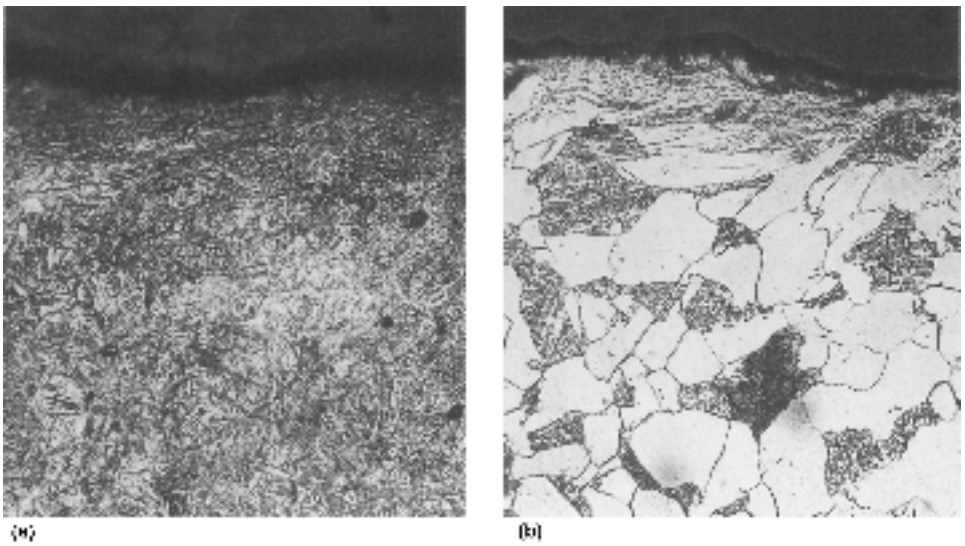

Fig. 92 Effect of hardening by plastic deformation. (a) Case-hardened surface. (b) Non-case-hardened surface. Both 243×. Source: Ref 30

process that plastically deforms the surface, producing increased surface compressive stresses. Figure 92 illustrates the formation of a case-hardened surface by shot peening (Ref 30).

Shot peening may also be used to remove directional machining marks. By masking, it is possible to localize this process to affect only the most critically stressed areas. The benefits may be lost if the initial surface is rough, and ragged surfaces may lead to folded-in defects.

Prior to conducting the peening process, the type of shot and the appropriate process parameters for the material and hardness must be determined. This may be done experimentally using an Almen strip. It is important that the shot are round, and the process must be precisely controlled to ensure complete coverage of the desired area.

Fatigue cracks generally initiate at the surface under bending conditions. Shot peening induces surface compressive residual stresses. Therefore, the possibility of fatigue crack initiation at the surface is reduced. A 20% improvement in fatigue limit or high-cycle fatigue life and contact-fatigue resistance has been quoted (Ref 30).

REFERENCES

1. S. Mocarski, Carburizing and Its Control, Part I: Basic Considerations, *Ind. Heat.,* Vol 41 (No. 5), 1974, p 58–70
2. A. Bavaro, Heat Treatments and Deformation, *Trait. Therm.,* Vol 240, 1990, p 37–41
3. F. Legat, Why Does Steel Crack during Quenching, *Kovine Zlitine Technol.,* Vol 32 (No. 3–4), 1998, p 273–276
4. R.W. Bohl, Difficulties and Imperfections Associated with Heat Treated Steel, Lesson 13, Heat Treatment of Steel, Materials Engineering Institute Course 10, ASM International, 1978
5. K.E. Thelning, *Steel and Its Heat Treatment,* Butterworths, London, U.K., 1985
6. H. Berns, "Distortion and Crack Formation by Heat Treatment of Tools," *Radex Rundsch.,* Vol 1, 1989, p 40–57
7. G. Beck, Internal Stresses Associated with Heat Treatment of Alloys, *Mém. Etud. Sci. Rev. Métall.,* June 1985, p 269–282
8. T. Ericsson and B. Hildenwall, Thermal and Transformational Stresses, *Sagamore Army Mater. Res. Conf., 28th Proc.,* 1981, p 19–38
9. C. Jensen, Dimensional Changes during Heat Treatment of Hot Work Steel, *Ind. Heat.,* March 1993, p 33–38
10. P. Mayr, "Dimensional Alteration of Parts due to Heat Treatment," *Residual Stresses in Science and Technology,* Vol 1, Garmisch-Partenkirschen, FRG, 1986, DGM Informationsgesellschaft mbH, Adenauerallee 21, D-6370, Oberursel, FRG 1987, p 57–77
11. R.W. Edmonson, Dimensional Changes in Steel during Heat Treatment, *Met. Treat.,* Vol 20 (No 6), 1969, p 3–19
12. M. Wisti and M. Hingwe, Tempering of Steel, *Heat Treating,* Vol 4, *ASM Handbook,* ASM International, 1991, p 121–136
13. Y. Toshioka, Heat Treatment Deformation of Steel Products, *Mater. Sci. Technol.,* Vol 1, 1985, p 883–892
14. T. Inoue, K. Haraguchi, and S. Kimura, Analysis of Stresses due to Quenching and Tempering of Steel, *Trans. Iron Steel Inst. Jpn.,* Vol 18, 1978, p 11–15
15. G.E. Totten and M.A.H. Howes, Distortion of Heat Treated Components, *Steel Heat Treatment Handbook,* G.E. Totten and M.A.H. Howes, Ed., Marcel Dekker Inc., 1997, p 292
16. D.A. Canonico, Stress-Relief in Heat Treating of Steel, *Heat Treating,* Vol 4, *ASM Handbook,* ASM International, 1991, p 33–34
17. C.E. Bates, G.E. Totten, and R.L. Brennan, Quenching of Steel, *Heat Treating,* Vol 4, *ASM Handbook,* ASM International, 1991, p 67–120
18. W.T. Cook, A Review of Selected Steel-Related Factors Controlling Distortion in Heat-Treatable Steels, *Heat Treat. Met.,* Vol 26 (No. 2), p 27–36
19. Y. Toshioka, Heat Treatment Deformation of Steel Products, *Mater. Sci. Technol.,* Vol 1, Oct 1985, p 1883–1892
20. A. Thuvander and A. Melander, Calculation of Distortion during Quenching of a Low Carbon Steel, *First ASM Heat Treatment and Surface Engineering Conference in Europe (Proc.),* Trans Tech Publications, Part 2, 1992, p 767–782
21. P.C. Clarke, Close-Tolerance Heat Treatment of Gears, *Heat Treat. Met.,* Vol 25 (No. 3), 1998, p 61–64
22. R.F. Kern, Thinking Through to Successful Heat Treatment, *Met. Eng. Q.,* Vol 11 (No. 1), 1971, p 1–4
23. R. Kern, Distortion and Cracking, Part II: Distortion from Quenching, *Heat Treat.,* March 1985, p 41–45
24. R. Kern, Distortion and Cracking, Part III: How to Control Cracking, *Heat Treat.,* April 1985, p 38–42
25. H.-J. Chen and Z.W. Jiang, Microstructure Improvement and Low-Temperature Quenching of Dies Made of Cr12-Type Steel, *Jinshu Rechuli,* No. 8, 1992, p 39–41
26. H.-H. Shao, Analysis of the Causes of Cracking of a 12% Cr Steel Cold Die during Heat Treatment, *Jinshu Rechuli,* No. 11, 1995, p 43
27. R.R. Blackwood, L.M. Jarvis, D.G. Hoffman, and G.E. Totten, Conditions Leading to Quench Cracking other than Severity of Quench, *Heat Treating, Including the Liu Dai Memorial Symposium, Proc. of the 18th Conf.,* R.A. Wallis and H.W. Walton, Ed., ASM International, 1998, p 575–585
28. F. Legat, "Why Does Steel Crack during Quenching," *Kovine Zlitine Technol.,* Vol 32 (No. 3–4), 1998, p 273–276
29. X. Cheng and S. He, Analysis of Quenching Cracks in Machine-Tool Pistons under Supersonic Frequency Induction Hardening, *Heat Treat. Met. (China),* No. 4, 1991, p 51–52
30. G. Parrish, *Carburizing: Microstructure and Properties,* ASM International, 1999
31. J.R. Davis, Ed., *ASM Materials Engineering Dictionary,* ASM International, 1992, p 407
32. P.F. Stratton, N. Saxena, and R. Jain, Requirements for Gas Quenching Systems, *Heat Treat. Met.,* Vol 24 (No. 3), 1997, p 60–63
33. H.M. Tensi, G.E. Totten, and G.M. Webster, Proposal to Monitor Agitation of Production Quench Tanks, *Heat Treating: Including the 1997 International Induction Heat Treating Symposium, Proc. of the 17th Conf.,* D.L. Milam, D.A. Poteet, G.D. Pfaffmann, V. Rudnev, A. Muehlbauer, and W.B. Albert, Ed., ASM International, 1997, p 423–441
34. S. Owaku, Quench Distortion of Steel Parts, *Netsu Shori (J. Jpn. Soc. Heat Treat.),* Vol 32 (No. 4), 1992, p 198–202
35. R.T. Von Bergen, The Effects of Quenchant Media Selection on the Distortion of Engineered Steel Parts, *Quenching and Distortion Control,* G.E. Totten, Ed., ASM International, 1992, p 275–282
36. H.M. Tensi, A. Stich, and G.E. Totten, Fundamentals of Quenching, *Met. Heat Treat.,* Mar/Apr 1995, p 20–28
37. T. Kunitake and S. Susigawa, *Sumitomo Search,* May 1971, p 16–25
38. V.D. Kalner and S.A. Yurasov, Internal Oxidation during Carburizing, *Met. Sci. Heat Treat. (USSR),* Vol 12 (No. 6), June 1970, p 451–454
39. A.A. Polyakov, Quenching Properties of Parts Having Stress Concentrators, *Met. Sci. Heat Treat.,* Vol 37 (No.7–8), 1995, p 324-325
40. A.G. Haynes, Interrelation of Isothermal and Continuous-Cooling Heat Treatments of Low-Alloy Steels and Their Practical Significance, *Heat Treat. Met.,* Special Report 95, The Iron and Steel Institute, 1966, p 13–23
41. D.P. Koistinen and R.E. Marburger, A General Equation Prescribing the Extent of the Austenite-Martensite Transformation in Pure Iron-Carbon Alloys and Plain Carbon Steels, *Acta. Metall.,* Vol 7, 1959, p 59–60
42. H. Webster and W.J. Laird, Jr., Martempering of Steel, *Heat Treating,* Vol 4, *ASM Handbook,* ASM International, 1991, p 137
43. J.R. Keough, W.J. Laird, Jr., and A.D. Godding, Austempering of Steel, *Heat Treating,* Vol 4, *ASM Handbook,* ASM International, 1991, p 152–163
44. N.I. Kobasko, M.A. Arpnov, G.E. Totten, and A.V. Sverdlin, Method and Equipment for Implementation of Intensive Quenching, *Heat Treating, Including the Liu Dai Memorial Symposium, Proc. of the 18th Conf.,* R.A. Wallis and H.W. Walton, Ed., ASM International, 1998, p 616–621

45. I.Y. Arkhipov, V.A. Batyreva, and M.S. Polotskii, Internal Oxidation of the Case on Carburized Alloy Steels, *Met. Sci. Heat Treat. (USSR),* Vol 14 (No. 6), 1972, p 508–512
46. W.E. Dowling, W.T. Donlon, W.B. Copple, and C.V. Darragh, Fatigue Behavior of Two Carburized Low-Alloy Steels, *Proc. of Second International Conference on Carburizing and Nitriding with Atmospheres,* ASM International, 1995, p 55–60
47. B. Liscic, Heat Treatment of Steel, *Steel Heat Treatment Handbook,* G.E. Totten and M.A.H. Howes, Ed., Marcel Dekker, 1997, p 527–662
48. R. Ruxanda and E. Florian, Microscopic Observations of the Carbide/Matrix Interphasic Interface in a Low-Alloyed Hypercarburized Steel, *Proc. of Second International Conference on Carburizing and Nitriding with Atmospheres,* ASM International, 1995, p 117–121
49. J. Wang, Z. Qin, and J. Zhou, Formation and Properties of Carburized Case with Spheroidal Carbides, *5th International Congress on the Heat Treatment of Materials,* (Budapest), International Federation for Heat Treating and Surface Engineering (Scientific Society for Mechanical Engineering), 1986, p 1212–1219
50. J.G. Wang, Z. Feng, and J.C. Zhou, Effect of the Morphology of Carbides in the Carburizing Case on the Wear Resistance and the Contact Fatigue of Gears, *J. Mat. Eng. (China),* Vol 6, Dec 1989, p 35–40
51. R. Kern, Supercarburizing, *Heat Treat.,* Oct 1986, p 36–38
52. M.I. Vinograd, I.Y. Ul'Yanina, and G.A. Faivilevich, Mechanism of Austenite Grain Growth in Structural Steel, *Met. Sci. Heat Treat. (USSR),* Vol 17 (No. 1–2), 1975
53. R.P. Brobst and G. Krauss, The Effect of Austenite Grain Size on Microcracking in Martensite of an Fe-1.2C Alloy, *Metall. Trans.,* Vol 5, Feb 1974, p 457–462
54. J. Hewitt, The Study of Hydrogen in Low Alloy Steels by Internal Friction Techniques, *Hydrogen in Steel,* Special Report 73, The Iron and Steel Institute, 1962, p 83–89
55. T.A. Balliet and G. Krauss, The Effect of the First and Second Stages of Tempering of Microcracking in Martensite of an Fe-1.2C Alloy, *Metall. Trans. A,* Vol 7, Jan 1976, p 81–86